

63-34
2102

FORWARDED BY THE CHIEF, BUREAU OF SHIPS

404193



TYCO LABORATORIES, INC.

BEAR HILL, WALTHAM 54, MASSACHUSETTS
AREA CODE 617
TELEPHONE: 899-1650

CATALOGED BY ASTIA
AS AD FIG.

Interim Report

POWER DENSE THERMOELECTRIC MODULE

Covering Period

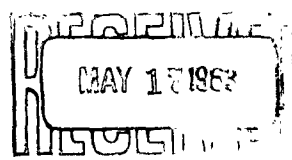
July 3, 1961 - November 2, 1962

THIS DOCUMENT MAY BE RELEASED WITH NO
RESTRICTIONS ON DISSEMINATION

Prepared For:

BUREAU OF SHIPS, DEPARTMENT OF THE NAVY

Contract Nobs-86015
Index No. SF - 01306



Edited by
Martin Weinstein

TABLE OF CONTENTS

	<u>Page</u>
I. Introduction	1
II. The Bonding of Lead Tellurides	2
A. Diffusion Bonding of N-Type Lead Telluride to Pure Iron Electrodes	2
B. Braze-Bonding of P-Type Lead Telluride to Pure Iron Electrodes	5
C. Alternate Braze-Bonding Procedure for N-Type Lead Telluride	15
D. The Design, Construction and Electrical Evaluation of Braze-Bonded Lead Telluride Thermocouples	18
III. Materials Development	29
A. General Remarks Concerning the Effects of Ultrasonic Oscillations on the Crystallization of Molten Metals	29
B. Design and Construction of Equipment	29
C. Experimental Procedure	32
D. Experimental Results	32
E. The Thermoelectric Properties	33
F. Electrical Properties as a Function of Temperature	40
1. Resistivity	40
2. Seebeck Coefficient	40
3. Electrical Efficiency	45
G. Mechanical Properties of N-Type PbTe	45
1. Ductility	45
2. Ultimate Compressive Strength	47
H. Hot Pressing of Lead Telluride	50
IV. Effect of Thermal Gradients	52
A. Experimental Equipment	52
B. Experimental Results	52

	<u>Page</u>
V. Summary	58
VI. References	59
VII. Appendix I - Detailed Description of Bonding Process	60
VIII. Appendix II - Chemical Polish and Electrolytic Etch for PbTe	63
IX. Technical Contributors	65

LIST OF FIGURES

	<u>Page</u>
1. Diffusion Bonding Equipment	3
2. Photomicrograph of Fe- N-Type (PbI_2 -doped) PbTe Bond	4
3. Photomicrograph of Bond Region Prepared Using A Sb_2Te_3	6
4. Braze Bonding Set-up	7
5. Photomicrograph of Fe-SnTe-PbTe Composite	8
6. Resistance Profile of Fe-SnTe Couple	9
7. Resistance profile of SnTe - PbTe Couple	10
8. Resistance of Bonded and Unbonded P-Type PbTe (0.250" dia. x 0.0250" long) as a Function of Temperature	12
9. Resistance Profile of SnTe-PbTe Couple	13
10. Crack Formation in PbTe-SnTe Region After Heat Treatment	17
11. Thermocouple Testing Equipment	19
12. Voltage Output as a Function of Temperature for TLI Thermocouple	24
13. Total Resistance as a Function of Temperature for Thermocouple	25
14. Voltage Output as a Function of Time for TLI Thermocouple	27
15. Total Resistance as a Function of Time for TLI Thermocouple	28
16. Apparatus for Directional Solidification with Ultrasonic Irradiation	30
17. Quartz Container and Tool Coupling	31
18. Photomicrographs of Ultrasonically Irradiated Ingot	34
19. Photomicrographs of Directionally Solidified Ingot	35
20. Photomicrographs of Extruded PbTe	36
21. Photomicrograph of Cold Pressed and Sintered PbTe	37

	<u>Page</u>
22. Room Temperature Resistance Profile of Directionally Solidified PbTe and Irradiated PbTe	39
23. Resistivity as a Function of Temperature for N-Type PbTe	42
24. Voltage Output as a Function of Temperature for N-Type PbTe	43
25. Seebeck Coefficient as a Function of Temperature for N-Type PbTe	44
26. Electrical Efficiency α^2/ρ as a Function of Temperature for N-Type PbTe	46
27. Stress-Strain Relationships for N-Type PbTe	48
28. Photomicrograph of Hot Pressed PbTe	51
29. Thermal Gradient Testing Equipment	53
30. Life Test of N-Type PbTe	55
31. Life Test of Bonded N-Type PbTe	56

LIST OF TABLES

	<u>Page</u>
1. Electrical Properties of Fe-PbTe (P-Type)-Fe Thermo- elements (SnTe Intermediate)	14
2. Effect of Thermal Cycle	16
3. Electrical Properties of TLI Fabricated Thermocouple as a Function of Temperature	21
4. Room Temperature Seebeck Coefficients	41
5. Ultimate Compressive Strength (to Fracture) and Grain Size of N-Type PbTe	49
6. Thermal Gradient Test Results	54

I. INTRODUCTION

The basic objective of this study was to optimize the power to weight ratio of a lead telluride thermoelectric generator module. In order to accomplish this, it became apparent that certain improvements in the basic technology of lead telluride would be necessary. The three basic materials areas covered were:

1. A study of the bonding techniques to N and P-type lead telluride.
2. A materials preparation study involving the use of various metallurgical techniques such as hot pressing and directional solidification under the influence of ultrasonic irradiation. The aim of this segment of the work was to obtain polycrystalline aggregates of lead telluride with superior mechanical and electrical properties.
3. A study to determine the effects of temperature gradients on the thermoelectric and mechanical properties of bonded and unbonded lead telluride thermoelements.

II. THE BONDING OF LEAD TELLURIDE

A major limitation to the efficiency of lead telluride thermocouples is the contact resistance at the interface of lead telluride with metal electrodes. Various techniques have been used to reduce contact resistance such as compression loading at the hot junction together with soft soldering of the cold junctions.⁽¹⁾ Even with these mechanically complex techniques, the contact resistance still contributes excessively to the total resistance of the thermocouples. Since metallurgical bonds between the thermoelements and the electrode are obviously desirable, various techniques for bonding N and P-type lead telluride to an inert electrode, in this particular case pure iron, have been studied.

A. DIFFUSION BONDING OF N-TYPE LEAD TELLURIDE TO PURE IRON ELECTRODES⁽²⁾

Standard (PbI₂-doped)N-type PbTe has been bonded to pure iron electrodes by interdiffusion at $858 \pm 2^{\circ}\text{C}$ for 20 to 30 minutes. This temperature is 15°C below the PbTe - Fe eutectic, and therefore avoids the melting and recrystallization of lead telluride close to the junction. A dead weight axial loading of about 500 grams per cm² assists in plastic deformation of lead telluride so that it conforms to the contours of the electrode surface. The experimental set-up is shown in Figure 1.

The other experimental requirements for bonding are that the parts be scrupulously clean and that the bonding ambient contain less than 2 or 3 parts per million of oxygen. Figure 2 shows the interface region of a typical bond. The bonds in almost all cases had a contact resistance of less than 10 micro-ohm-cm² and were mechanically stronger than the lead telluride itself. They also did not deteriorate in mechanical or thermoelectric properties during extended life tests at operating temperature. The majority of deterioration found on extended life tests at operating temperature was due to the deterioration of the lead telluride itself. It should be kept in mind, however, that slight oxygen potentials in the ambient system will cause failure by intergranular corrosion.

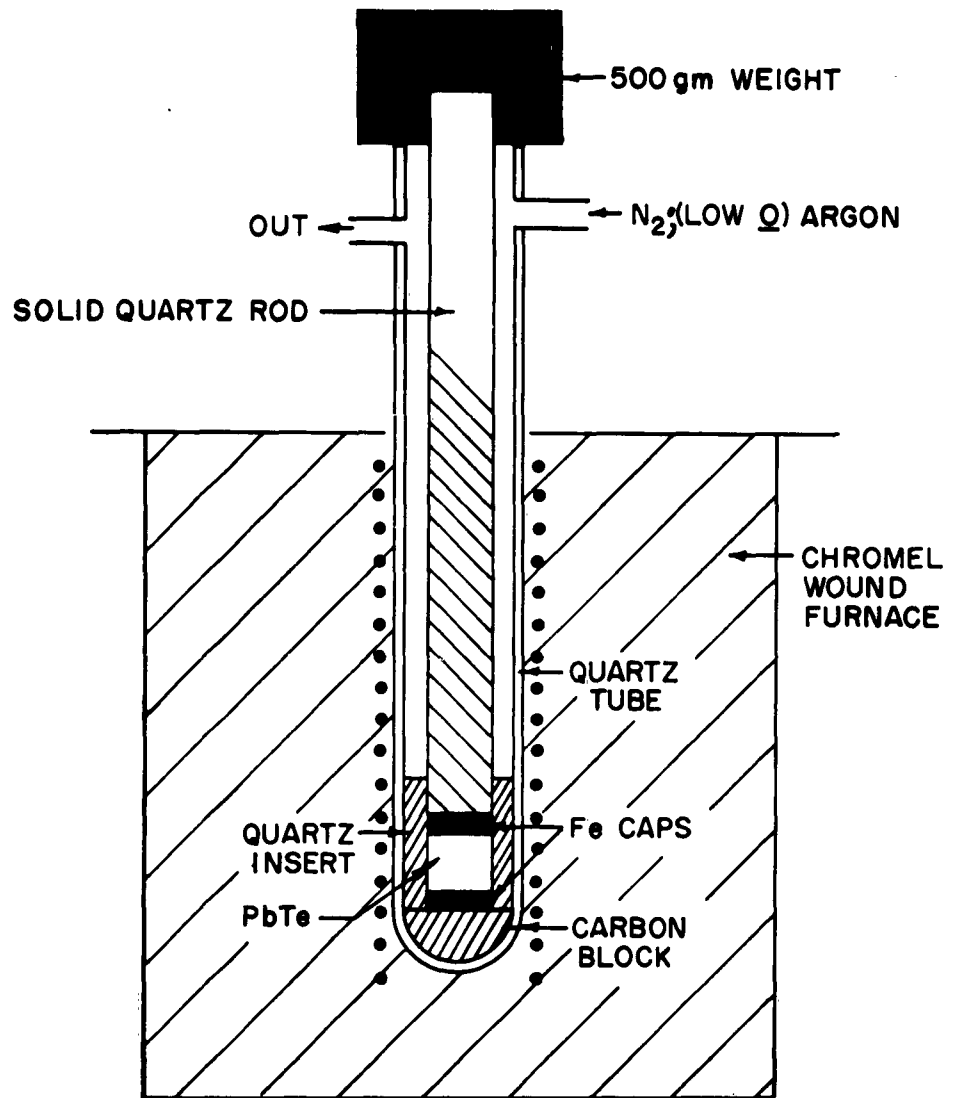


FIG. 1 DIFFUSION BONDING EQUIPMENT

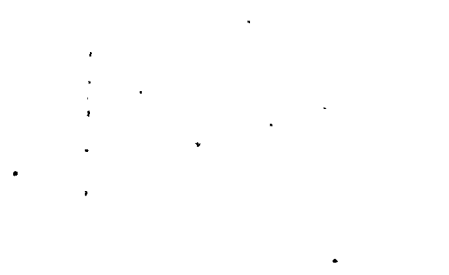


FIGURE 2 - PHOTOMICROGRAPH OF Fe- N-TYPE (PbI₂-doped)
PbTe BOND 300 X

The thermoelectric properties of bonded N-type thermoelements will be reported both as a function of temperature and time in a subsequent section. A thorough description of the diffusion bonding process is given in Appendix I.

B. BRAZE BONDING OF P-TYPE LEAD TELLURIDE TO PURE IRON ELECTRODES⁽²⁾

We were unable to obtain satisfactory diffusion bonds of iron to Na doped P-type lead telluride, therefore, an alternate approach utilizing an intermediate brazing material was explored. The criteria underlying our choice of braze were that it bond independently to iron and to P-type lead telluride, that it have an intrinsically high electrical conductivity, that its melting point lie between the upper operating temperatures of the thermocouple and melting point of lead telluride, that it form a graded region in the vicinity of the bond to minimize strains from the mismatch in expansion coefficient, and that it not cause chemical or electrical deterioration of lead telluride at operative temperatures.

These criteria lead us to investigate the use of P-type semi-metals of crystal structures related to that of lead telluride. Antimony telluride was found to be unsuitable as it yielded a highly resistant two-phase region at the junction with lead telluride. The two phase region is clearly shown in Figure 3. The bonding equipment used is shown in Figure 4. Germanium telluride was also found to be unsuitable since it did not wet iron. We have, however, achieved excellent bonds using tin telluride. The equipment used is shown in Figure 4. Tin telluride readily wets iron and also forms a complete series of solid solutions with lead telluride. It can be seen in Figure 5 that tin telluride penetrates the iron intergranularly and that tin telluride and lead telluride form a completely graded solid solution. Resistance profiles for iron - SnTe and SnTe - PbTe couples are shown in Figures 6 and 7 respectively. As can be seen, there is negligible resistance increase at the interface of these couples, and that SnTe appears to possess almost metallic conductivity at room temperature.

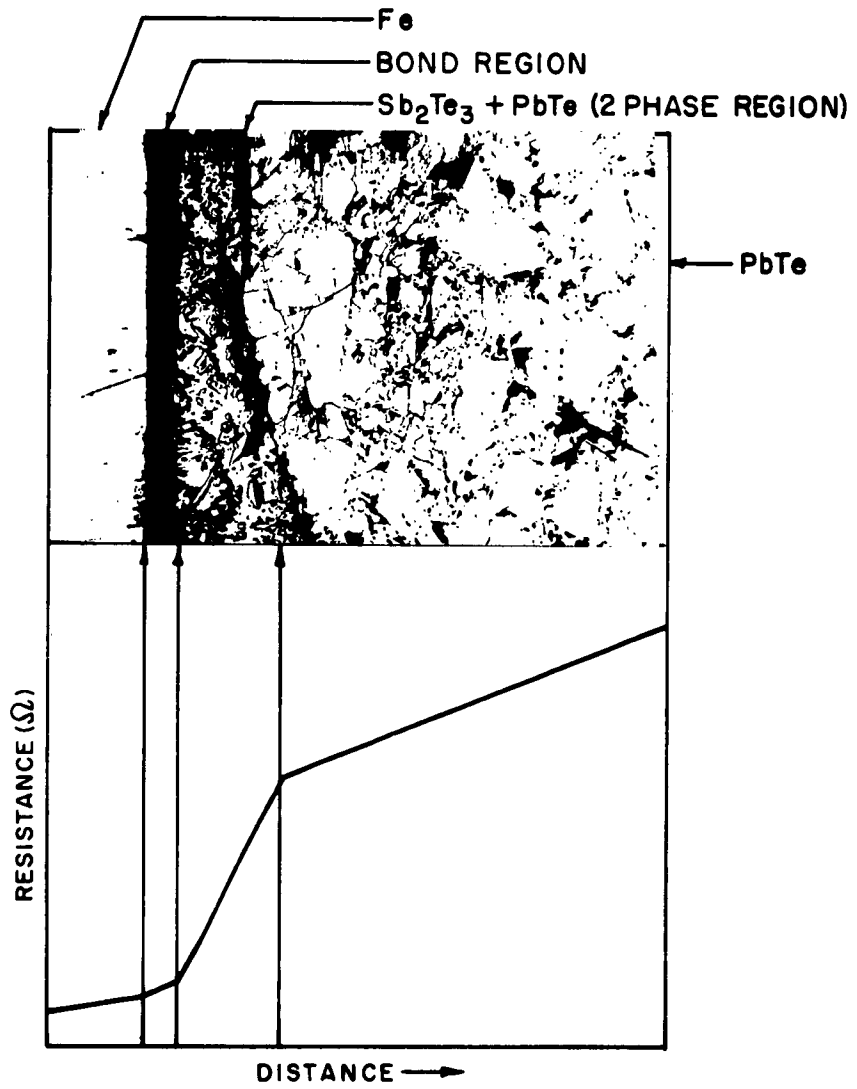


FIG. 3 PHOTOMICROGRAPH OF BRAZE BOND USING Sb_2Te_3

- A-ARGON
- B-NEEDLE VALVE
- C-STOPCOCK
- D-BUBBLER
- E- DRYING TOWER
- F- COPPER FURNACE
- G- MANOMETER
- H- VACUUM TRAP
- I- VACUUM PUMP
- J- RUBBER BUNG
- K- QUARTZ TUBE (5' LONG)
- L- RESISTANCE FURNACE
- M- CARBON JIG
- N- STAINLESS STEEL WEIGHT

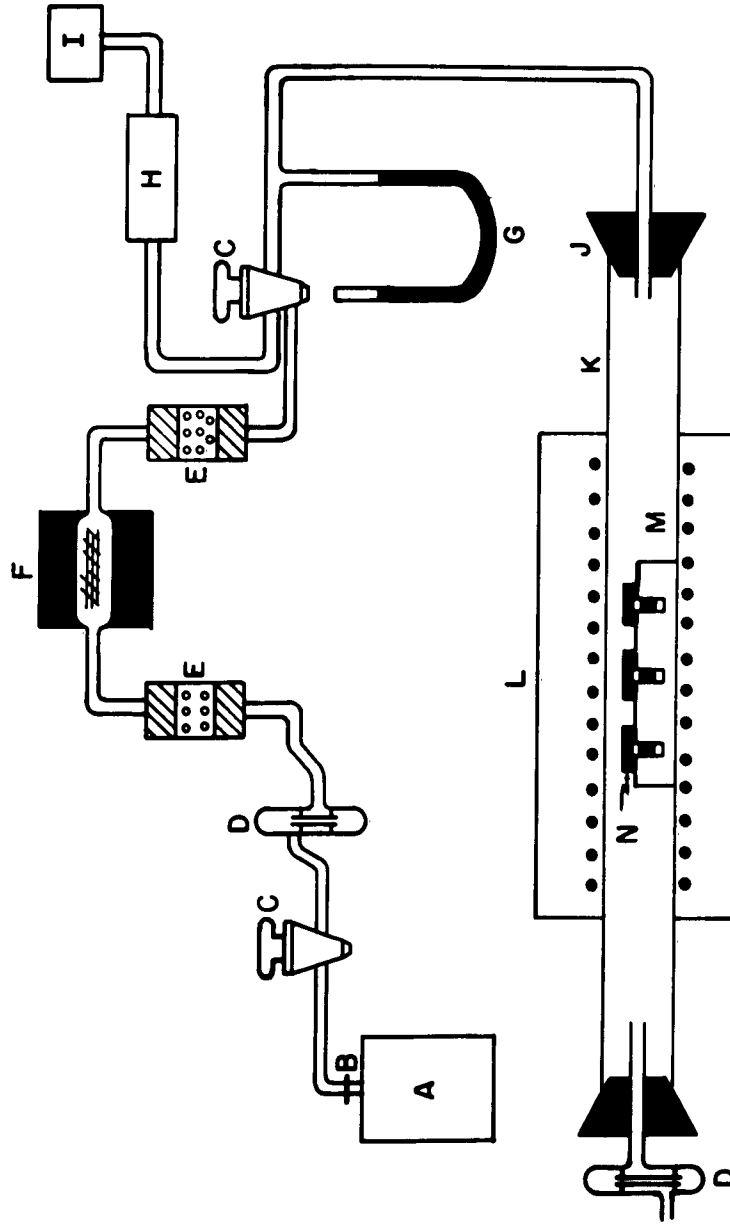


FIG. 4 BRAZE BONDING EQUIPMENT



FIGURE 5 - PHOTOMICROGRAPH OF Fe-SnTe-PbTe COMPOSITE
200 X

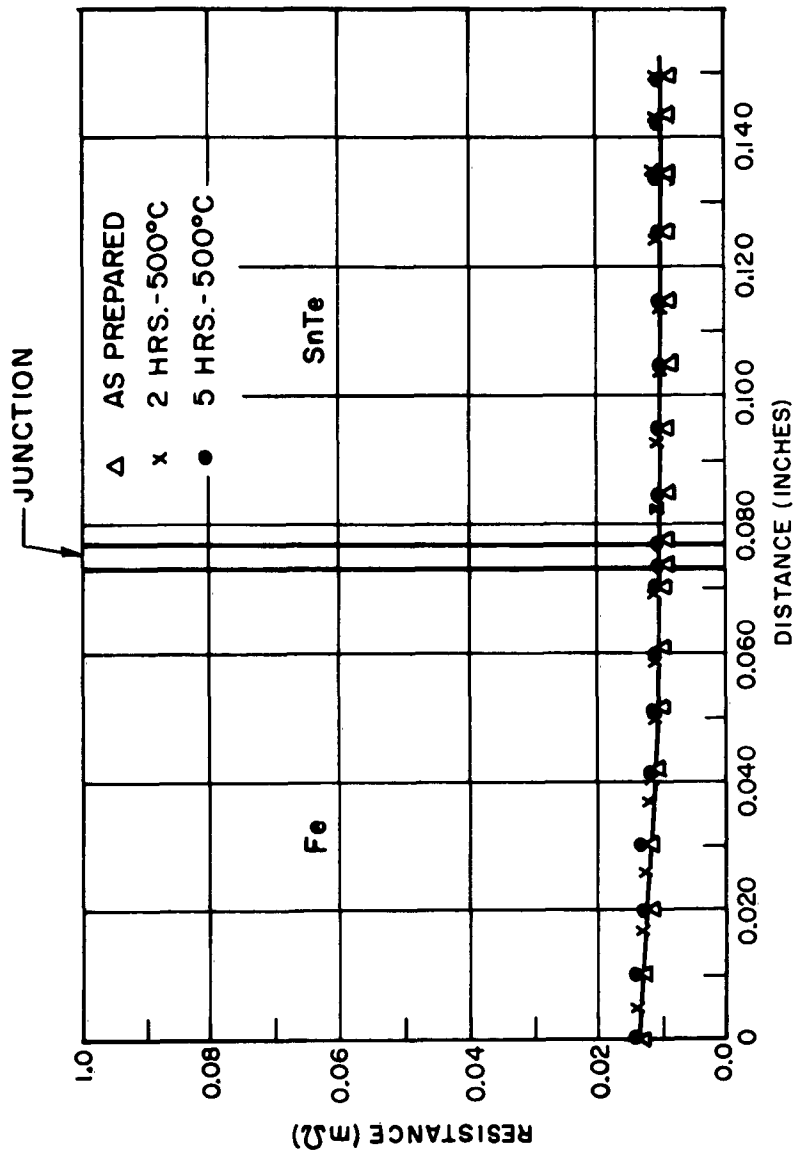


FIG. 6 RESISTANCE AS A FUNCTION OF DISTANCE FOR Fe-SnTe COUPLE

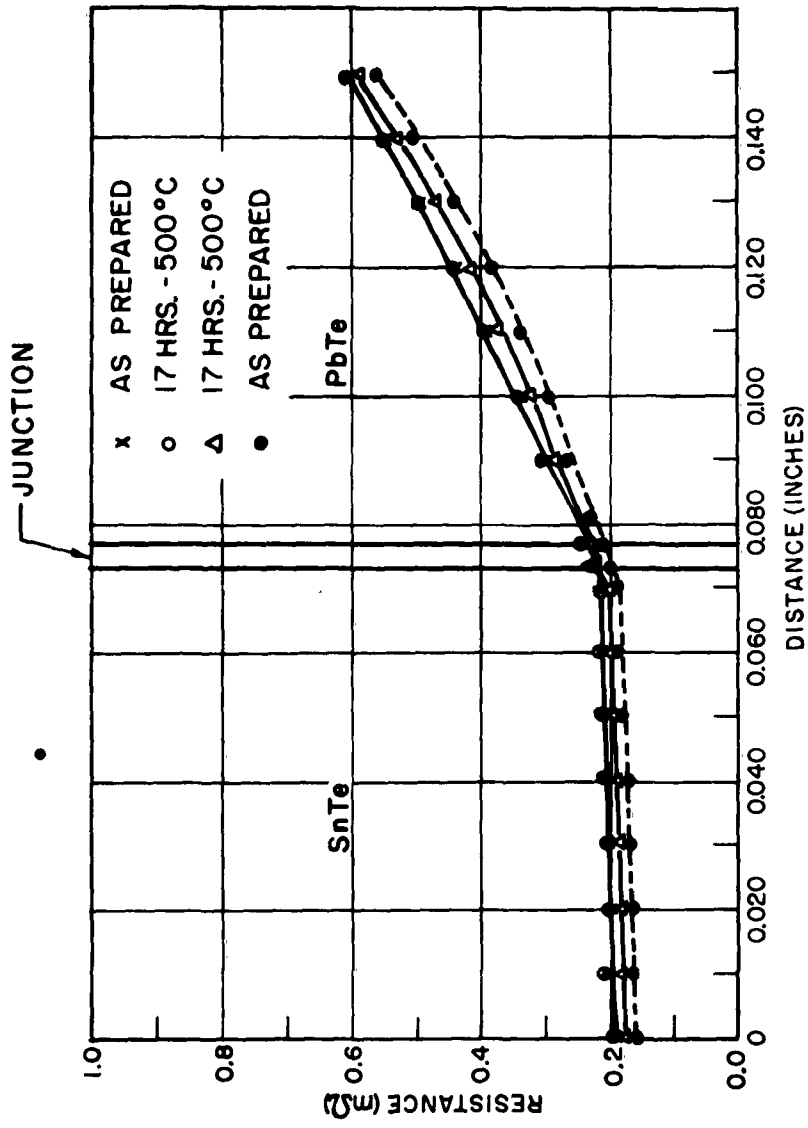


FIG. 7 RESISTANCE AS A FUNCTION OF DISTANCE FOR SnTe-PbTe COUPLES

In practice, pure stoichiometric SnTe must be used. We found it necessary to zone-level ingots of stoichiometric SnTe several times before a constant melting point was achieved. This was found to be $805 \pm 2^{\circ}\text{C}$, which is approximately 15°C higher than that reported previously. (3) The bond is prepared in two steps. Firstly, powdered SnTe is applied to pure iron electrodes by melting it on at 850°C for about one hour; excess SnTe is then ground off leaving about 4 mils on the electrode. Secondly, the PbTe thermoelement is bonded to the Fe-SnTe composite at 808°C for two (2) to four (4) minutes. As in preparing the N-type diffusion bonds, scrupulous attention to the cleanliness of the parts, and to the use of oxygen-free ambients, is necessary.

Properly prepared bonds have values of contact resistance typically 10 micro-ohm-cm² of less, and have excellent mechanical strength. Figure 8 shows the variation with temperature of the total resistance of a PbTe thermoelement (1/4 inch in diameter by 1/4 inches long) bonded to iron electrodes on both ends. The resistance of an unbonded thermoelement on the same dimensions is shown for comparison. It can be seen that the resistance of the doubly bonded thermoelement is less than that of the unbonded one over much of the temperature range. This difference is attributable to the random variation of the properties of P-type PbTe from sample to sample. A voltage output of approximately 120 millivolts was observed for both samples when supported between a source at 550°C and a heat sink at 20°C . The combination of the resistance values and the voltage output indicates that the bonds do not reduce the thermoelectric conversion efficiency.

The bond is susceptible to oxidation both during fabrication and operation. However, heating separate Fe-SnTe and SnTe-PbTe couples at 550°C for more than 500 hours in an oxygen free ambient produced no deterioration of the bond regions (See Fig. 9). A slight migration of the SnTe - PbTe interface was observed. This amounted to about 0.001 inches and was complete within the first 20 hours of heating.

Since oxygen was found to be a prime culprit in the deterioration of the bond region, the effect of oxidation and heat treatment on the electrical properties of Fe-SnTe - PbTe composite thermoelements have been investigated. The pertinent data may be found in Tables I and 2. In some

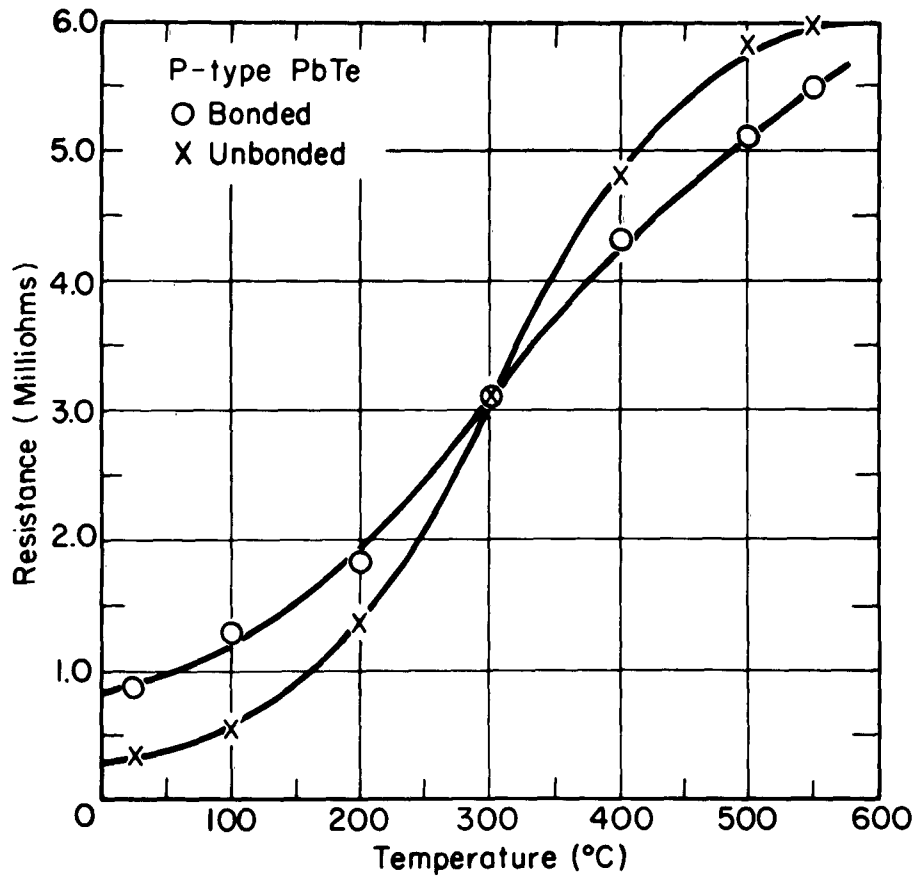


Fig. 8 The resistance of bonded and unbonded p-type PbTe (0.250" diam. x 0.250" long) as a function of temperature

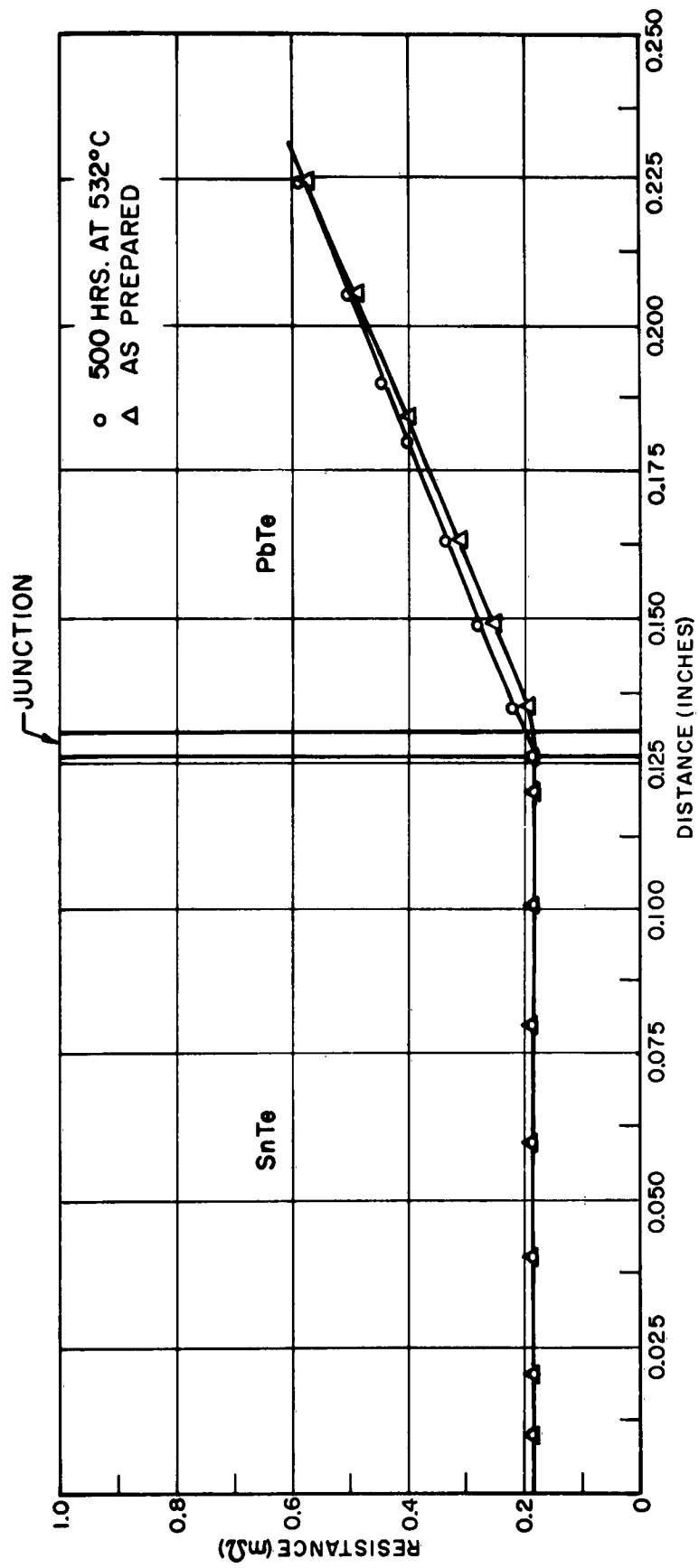


FIG. 9 RESISTANCE VS DISTANCE PROFILE OF SnTe - PbTe COUPLE

TABLE 1 - Electrical Properties of Fe-PbTe(P-Type) Fe Thermoelements (SnTe Intermediate)

Double Bond #	Total Resistance milliohms (R. T.)		Resistivity milliohm-cm (R. T.)		Room Temperature Seebeck Coeff. $mv \times 10^{-3}/^{\circ}C$		Voltage Output (mv)	
	Initial	After 134 Hrs. at 550°C	Initial PbTe Supplied	Final (assuming no contact resistance)	Initial	Final	Initial PbTe Supplied	Thermoelement after 134 hrs.
1	2.4	2.41		1.2	52	50.1		
2	1.3	1.4		0.65	49	47.0	110	
3	1.9	1.93		1.0				
4	1.4	1.5		0.7	63	76.6		
5	1.5	4.0#		2.0	30	39.5		135
6	1.5	4.0#	0.209	2.0	43	45.5	120	110
7			0.318		43.7	57.1	112	
8	2.1*	10	0.328	5	48.9	30.0	124	130
9	2.2*		0.177	1.1		63.5	121	
10	2.2	2.55	0.256	1.2			126	
11	1.6	1.6	0.498				111	
12	2.40							
13	1.40* (slow Cool)							

* Vacuum used to remove porosity

Resistance increase after 5 min. in voltage output apparatus - oxidation

cases, slight oxidation caused a two-fold increase in resistivity. In order to differentiate between the effects of thermal treatment and of oxidation on P-type lead telluride, a system was constructed which allowed the preparation of the bonds to take place in a high purity ambient. Using this system, no trace of oxidation was present on the surface of the iron electrodes, thereby substantiating the absence of even slight oxygen potentials.

The electrical properties of PbTe were found to be extremely sensitive to thermal treatment. A sample of P-type PbTe given exactly the same treatment as the bonded P-type PbTe increased in resistivity from 0.24 milli-ohm-cm to 0.45 milli-ohm-cm. Re-evaluation of data obtained from the PbTe - SnTe couple investigation showed the average resistivity of PbTe after bonding to be approximately 0.58 milli-ohm-cm. The resistivity remained constant with further heating at 550°C. Table 2 illustrates the effect of thermal cycling on the resistivity of thermoelements. It is apparent from this data that the effect of previous heat treatment may contribute more to the change of resistivity of the composites than the sum of all other effects. It should be noted that the PbTe itself continued to decrease in resistivity during the annealing treatment. The subsequent increase in resistivity present in the thermoelements was due to oxidation of the bond, and in a few cases, the formation of micro-cracks caused by differences in thermal expansion of the composite materials. Though crack formation was rare, it did in some cases interfere with resistance measurements. The cracks appeared to form in the bulk PbTe and to propagate to the PbTe -SnTe region (See Figure 10).

C. ALTERNATE BRAZE-BONDING PROCEDURE FOR N-TYPE LEAD TELLURIDE

Because of the unique brazing properties of SnTe, the process described above for P-type was applied to N-type material. The bond so formed had excellent mechanical properties but had high resistances. However, it was found that an alloy consisting of 1% by weight of iron in SnTe gave excellent results.

The process used for N-type PbTe is identical to that for P-Type PbTe with one exception, that of the addition of one percent by weight of iron to the brazing compound. This alloy was found to be single phase with a melting point approximately that of pure tin telluride. The reasons for the

TABLE 2 Effect of Thermal Cycle - Anneal @ 650°C and Furnace Cool (5 hrs. 40°C)

Sample #	Initial Resistance	1 hr. @ 650°C	2hrs. @ 650°C	18 hrs. @ 650°C
1	2.41 Ω	1.55 ¹ Ω	4.40 ² Ω	6.00 ³ Ω
3	1.93	5.70 ²		3.60 ³
10	2.55	1.55 ¹	4.00 ²	6.90 ²
12	2.40	2.14 ¹	2.60 ²	3.00 ³
20	1.40	2.20 ²		2.30 ³

PbTe (Trancoa)				
(as supplied)	= 0.652 x	0.4 x 10 ⁻³	0.448 x 10 ⁻³	0.287 x 10 ⁻³
= 0.252 x 10 ⁻³	10 ⁻³ ohm-cms	ohm-cms	ohm-cms	ohm-cms

1. Flowing H₂-Argon atmosphere - slight Fe oxidation visible.
2. Encapsulated with Argon - no visible oxidation.
3. Flowing N₂-H₂ - slight Fe oxidation.

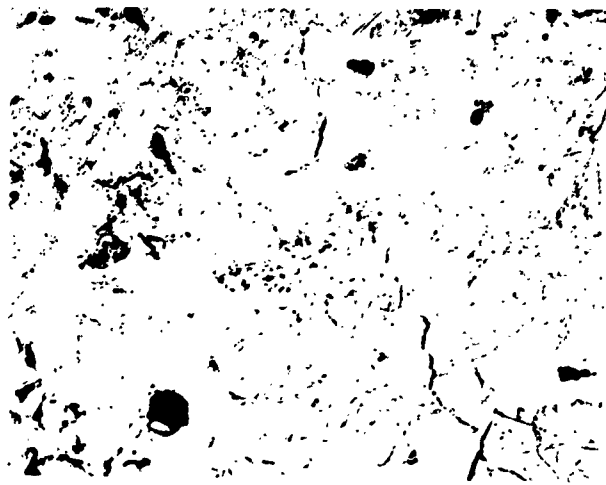


FIGURE 10 - CRACK FORMATION IN PbTe REGION AFTER HEAT TREATMENT

reduction of contact resistance using the 1% Fe alloy have not yet been determined. The advantage, of course, for this method over the diffusion bonding technique is simply that the same sample preparation, jiggling, time temperature cycles, etc., can now be used for both N and P-type lead telluride. The thermal expansion characteristics of both couples would now also be quite similar, thereby, reducing the possibility of micro-crack formation.

D. THE DESIGN, CONSTRUCTION AND ELECTRICAL EVALUATION OF BRAZE-BONDED LEAD TELLURIDE THERMOCOUPLES

In order to determine the operating characteristics of the bonded lead telluride thermoelements, the P and N legs were fabricated into thermocouple form. The thermocouple consisted of P and N-type lead telluride attached to iron conductors approximately 0.010 inches thick. The tin telluride composite braze material was 0.003 inches plus or minus 0.001 inches thick. The completed thermoelements were silver soldered to a copper strip 0.368 inches by 0.746 inches by 0.032 inches thick, using thin discs of Silvalloy 45.

Initial soldering attempts in which the copper strip and thermoelements were tightly clamped into a carbon enclosure were unsuccessful. In all cases, the lead telluride thermoelement cracked as a consequence of constrained thermal expansion. Since spring loading and dead weight loading involve various mechanical problems, an alternative procedure was utilized. Instead of using a tight clamp fit on the thermoelements, a synthetic high temperature spring, in this particular case a compressed section of steel filings, was placed at the bottom of the over-sized thermoelement enclosure. The steel filings were found to supply a sufficient amount of pressure for successful soldering without the previously accompanying damage to the thermoelements. Thirty (30) such thermocouples were fabricated.

A sketch of the thermocouple testing equipment is shown in Figure 11. The exterior fixture consists of a pyrex bell jar and an aluminum base plate. There are two Conax fittings in the base plate which allow the entry of two copper-constantan thermocouples and one chromel-alumel thermocouple. The copper-constantan thermocouples are permanently soldered

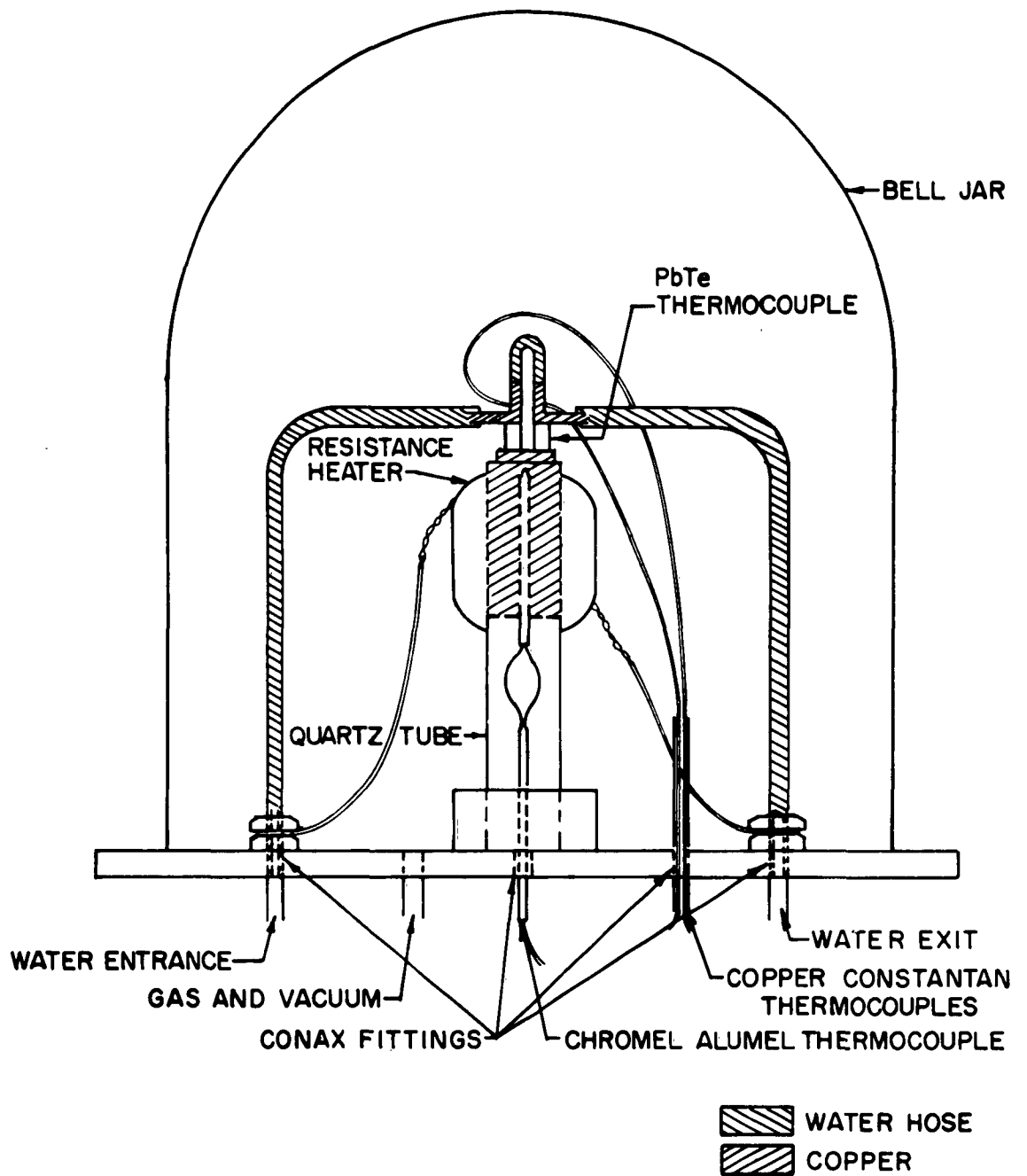


FIG. II THERMOCOUPLE TESTING DEVICE

to two water-cooled cold junction contacts. The thermocouples allow not only the measurements of the cold junction temperature, but they also allow the measurement of the total resistance and voltage output of the thermocouple. A chromel-alumel thermocouple which was a press fit to the copper connector strip, measured the hot junction temperature. Applying a suitable value of the average thermal conductivity to the above data, a value for the efficiency of the thermocouple may be obtained. The testing device is also suitable for life test studies. Heating of the thermocouple is accomplished by heating the copper bar which is located inside a long quartz retainer cylinder. Since a large volume of copper is available for heating, no trouble was encountered in obtaining the desired temperatures. The resistance and voltage output of the TLI fabricated thermocouples, are presented as a function of temperature and time. The appropriate data is given in Table 3. The voltage output and the total resistance as a function of temperature are shown in Figures 12 and 13, respectively. The initial voltage output and total resistance are those expected, given the manufacturer's specification of the thermoelements and our knowledge concerning the effects of the braze-bonding process. Slight deterioration of the PbTe thermocouple was observed with time. The initial efficiency of the thermocouple with $T_h = 539^\circ\text{C}$ and $T_c = 72^\circ\text{C}$ was calculated to be 9.55%. After 50 hours the efficiency decreased to value of 9.1%. Since there are many variations in the calculation of thermoelectric generator efficiencies a simple calculation is given below.

Data

$$T_H = 539^\circ\text{C}$$

$$T_C = 72^\circ\text{C}$$

$$\text{Voltage output} = 195 \text{ mv}$$

$$\text{Total resistance} = 11.20 \text{ m}$$

Thermocouple - Two Elements (P + N)

$$\alpha_{av} = \frac{195}{467 + 467} = 2.10 \mu\text{v}/^\circ\text{C}$$

$$\rho_{av} = \frac{11.20 \times 0.316}{1.270} = 2.785 \Omega\text{-cm} \times 10^{-3}$$

TABLE 3

Electrical Properties of TLI Fabricated Thermocouple
As Function of Temperature

<u>Temperature (T_H)</u>	<u>Resistance (mΩ)</u>	<u>Voltage Output (mv)</u>
20	2.93	0.30
32	3.06	2.00
45	3.12	4.60
70	3.40	9.40
78	3.50	11.50
89	3.55	14.00
94	3.60	14.95
98	3.69	16.25
102	3.74	17.25
107	3.79	18.20
113	3.94	20.50
121	4.00	22.40
128	4.10	24.25
135	4.30	26.00
139	4.35	27.25
142	4.45	28.00
154	4.76	33.00
168	5.05	38.00
179	5.13	42.00
189	5.30	45.00
197	5.45	49.00
200	5.48	50.00
215	5.75	55.00
218	5.80	56.25
224	5.90	58.00
228	6.0	60.00
235	6.3	63.00
239	6.4	64.00
247	6.4	68.10
248	6.45	69.00
253	6.50	71.80

<u>Temperature (T_H)</u>	<u>Resistance (m Ω)</u>	<u>Voltage Output (mv)</u>
257	6.60	73.90
262	6.70	75.50
270	6.90	79.00
273	6.95	80.00
276	7.00	81.50
284	7.15	85.00
292	7.40	88.00
296	7.50	90.00
300	7.60	92.00
305	7.75	95.00
315	7.95	97.00
319	8.00	100.00
322	8.20	103.00
325	8.35	105.00
332	8.35	107.50
335	8.40	109.50
341	8.55	112.50
346	8.7	115.00
355	8.9	120.00
363	9.1	125.00
370	9.15	128.00
385	9.50	135.00
394	9.60	140.00
404	9.50	145.00
408	10.1	147.00
412	10.30	150.00
424	10.45	155.00
428	10.50	158.00
433	10.70	160.00
445	10.70	165.00
454	10.90	170.00
465	10.95	175.00
475	11.00	180.00
484	10.90	185.00

<u>Temperature (T_H)</u>	<u>Resistance ($m\Omega$)</u>	<u>Voltage Output (mv)</u>
502	10.90	190.00
510	11.60	195.00
526	11.65	200.00
538	11.90	205.00
555	12.00	210.00
565	12.25	220.00
570	12.30	222.00

Note: $T_C = 15^\circ\text{C}$ 72°C (at $T_H = 500^\circ\text{C}$)

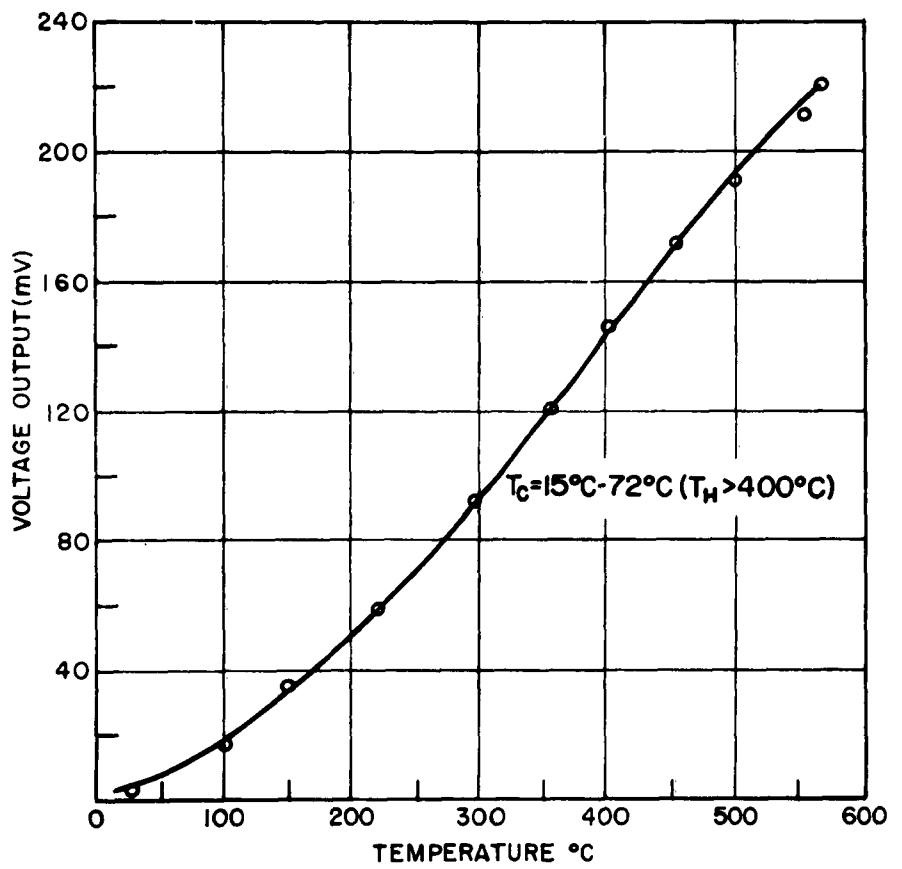


FIG. 12 VOLTAGE OUTPUT VS. HOT JUNCTION TEMPERATURE

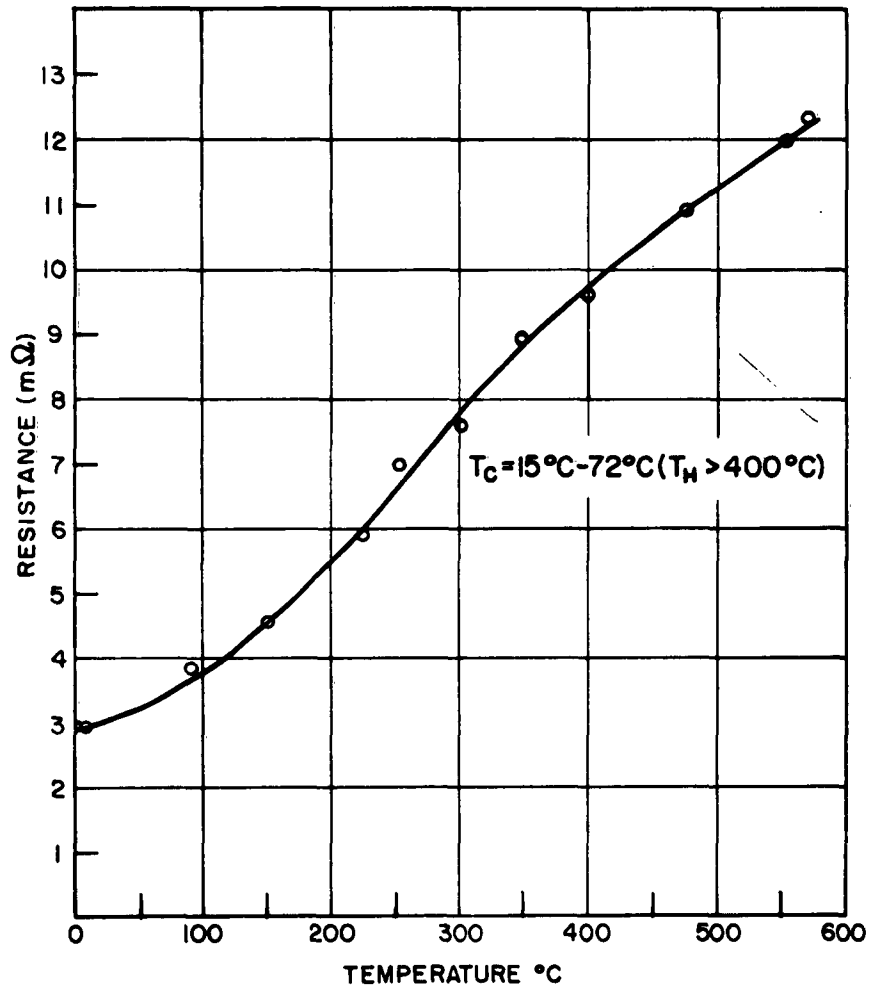


FIG. 13 RESISTANCE VS HOT JUNCTION TEMPERATURE

$$k_{av} = 0.016 \text{ w/cm}^{\circ}\text{C} \quad (\text{from published data})$$

$$Z = \frac{\alpha_{av}^2}{\rho_{av} k_{av}} = \frac{(2.10)^2}{1.6 \times 10^{-2} \times 2.785 \times 10^{-3}} = 0.988 \times 10^{-3}/^{\circ}\text{C}$$

$$M = 1 + 1/2 Z_{av} (T_C + T_H)$$

$$M = 1 + 1/2 (0.988) (1157) \times 10^{-3} = 1.253$$

$$\eta = \frac{T_H - T_C}{T_H} \times \frac{M - 1}{M + T_C/T_H}$$

$$\eta = \frac{812 - 345}{812} \times \frac{1.253 - 1}{1.253 + 345/812} = 9.55\%$$

An efficiency of 9.25% was obtained with $T_h = 571^{\circ}\text{C}$

After careful analysis it became apparent that the decrease of efficiency was mainly brought about by the deterioration of the P-type leg (Na-doped) of the thermocouple. The bond region was not effected, therefore, the major decrease in power output could be attributed to the lead telluride itself. Following our own observations, and those of other researchers in this field, we feel that the basic problem encountered with lead telluride thermocouples is involved with the intrinsic instability of sodium-doped PbTe. The voltage output and resistance $T_h = 539^{\circ}\text{C}$ and $T_c = 72^{\circ}\text{C}$ as a function of time are given in Figure 14 and 15, respectively. It may be seen that the major portion of deterioration occurred during the first fourteen hours of operation.

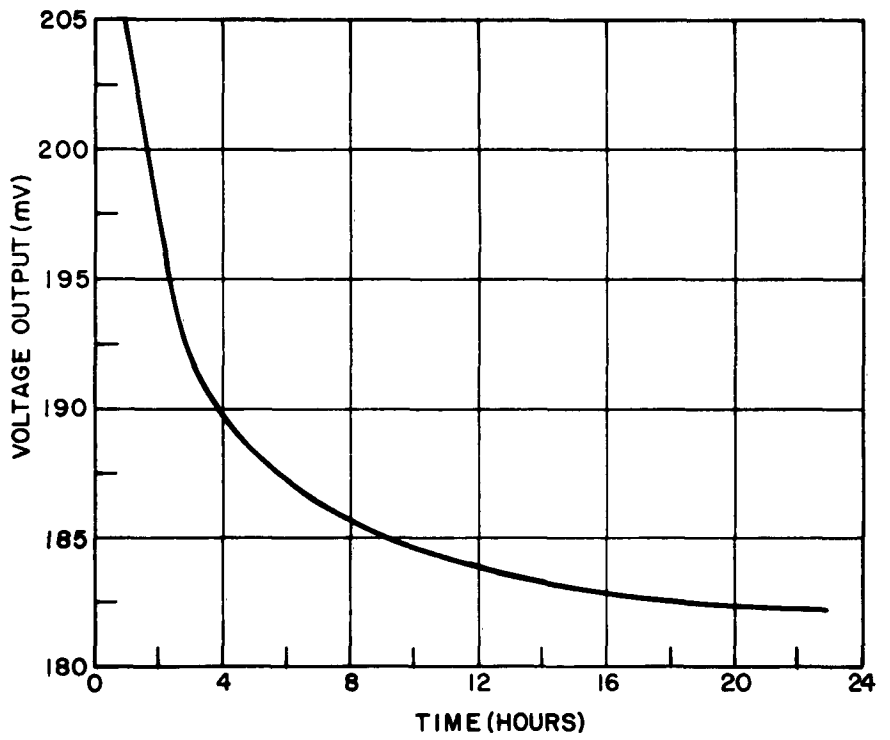


FIG. 14 VOLTAGE OUTPUT VS TIME

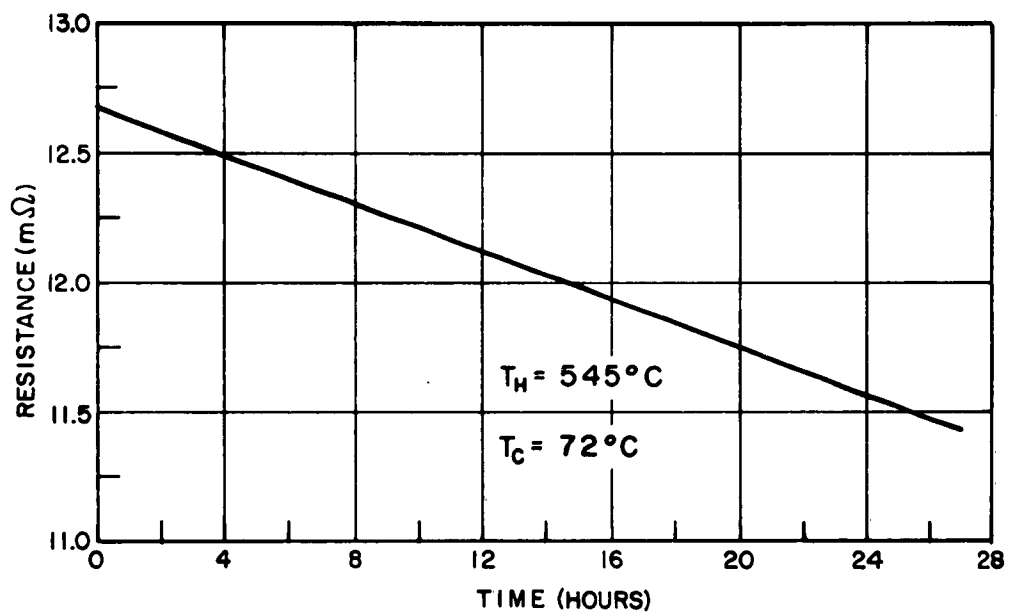


FIG. 15 RESISTANCE VS TIME

III. MATERIALS DEVELOPMENT

In this segment of the work various techniques for the fabrication of lead telluride thermoelements have been investigated. Work has concentrated on the preparation of the thermoelements by directional solidification under the influence of ultrasonic irradiation. Hot pressing techniques have also been studied.

A. GENERAL REMARKS CONCERNING THE EFFECTS OF ULTRASONIC OSCILLATIONS ON THE CRYSTALLIZATION OF MOLTEN METALS

The results of various investigations into the process of crystallization of molten metals demonstrates that ultrasonic oscillations can substantially improve the crystalline structure of a cast ingot. Both the mechanical properties and homogeneity of the ingot are improved. The mechanism of the ultrasonic effect on the crystallization of metals or alloys is primarily connected with the initiation of cavitation processes, which disrupt the growing solid-liquid interface. The ultrasonic waves are most effective in influencing the origination of crystallization centers during the formation of standing waves in the melt. In this case, at the nodes of the standing waves, origination and growth of crystals are possible. Additional crystallization centers may also appear as a result of transverse oscillations of the walls of the vessel in which the molten metal is contained. The dendritic crystals are also limited in their propagation by the frictional forces between the melt and the emerging dendrite. A program to investigate the effects of ultrasonic irradiation on the crystallization of PbTe was carried out.

B. DESIGN AND CONSTRUCTION OF EQUIPMENT

A schematic representation of the experimental equipment is shown in Figure 16. The ultrasonic oscillations were obtained using a Raytheon Impact Grinder, Model #2-332. The quartz ampule shown in Figure 17 was coupled to the ultrasonic oscillator by means of the modified tool mechanism shown. The use of ductile copper washers in contact with the quartz pedestal allowed an extremely tight fit between the glass assembly and the vibrating head. To investigate the effects of various rates of solidification on the final ingot structure, a modified Bridgeman

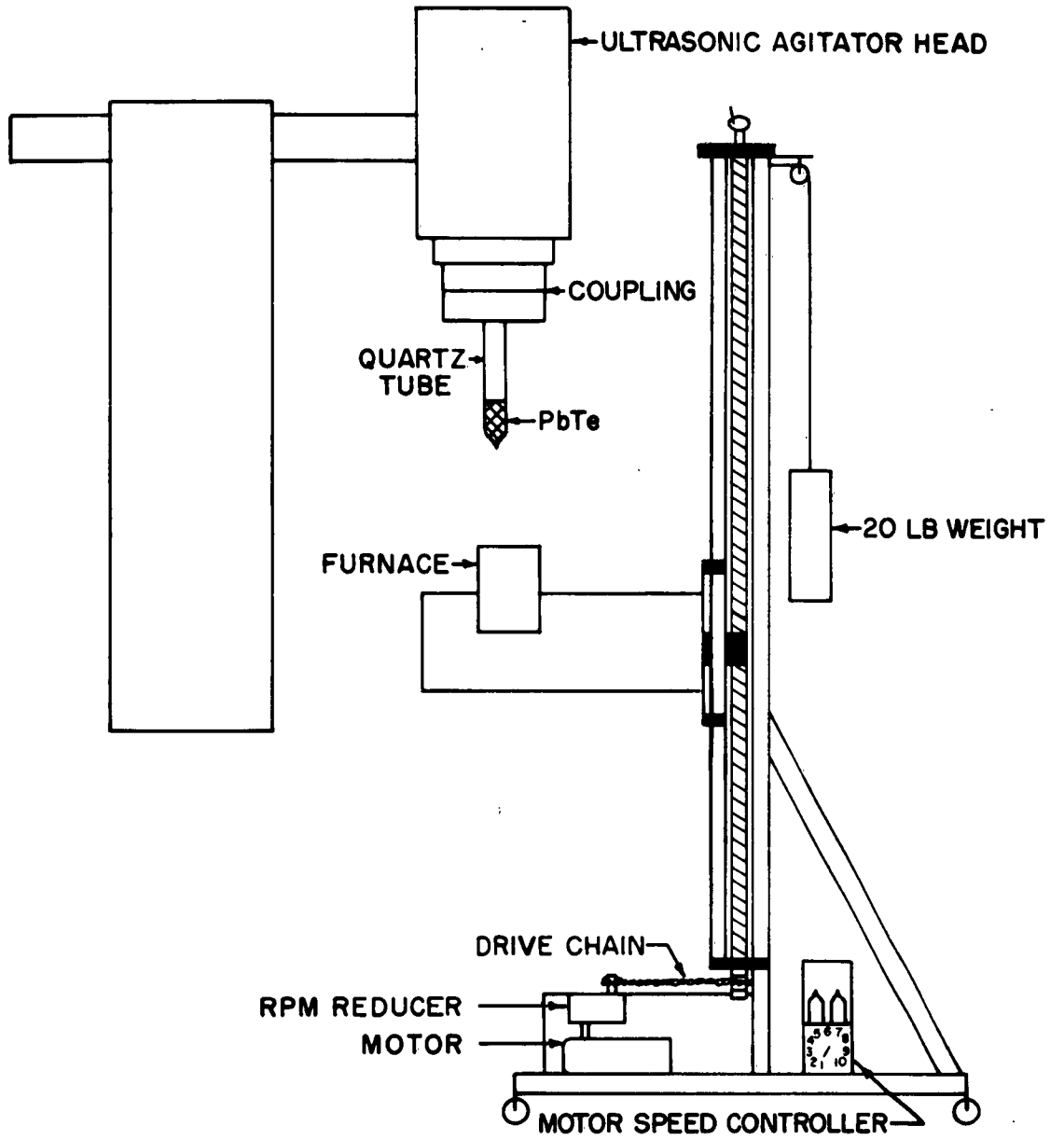


FIG.16 ULTRASONIC AGITATOR

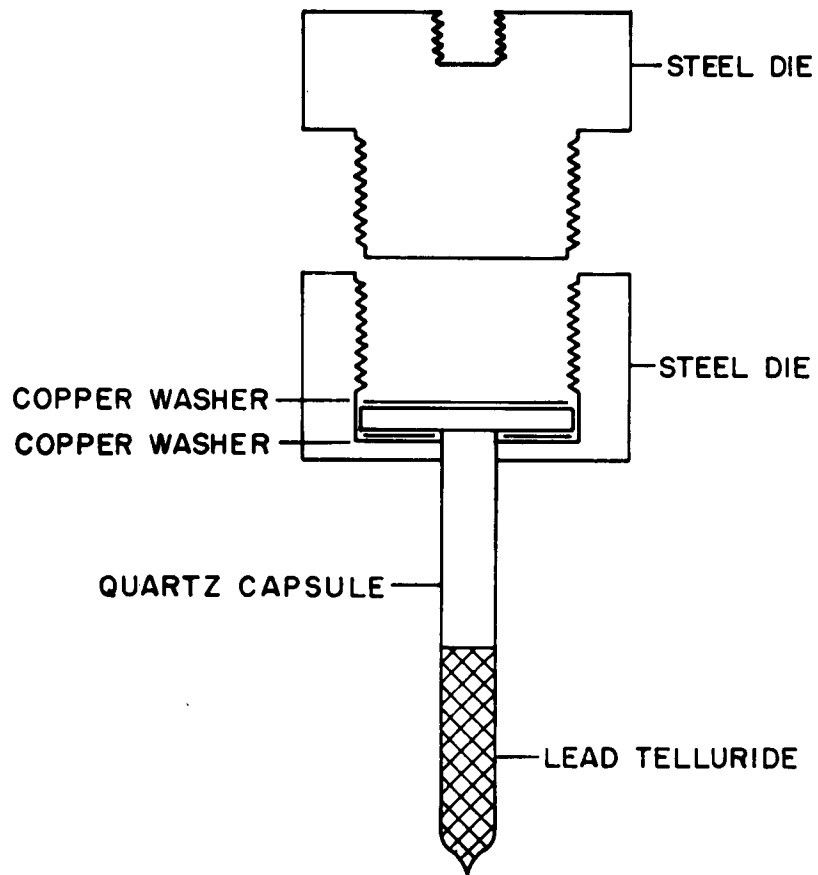


FIG. 17 COUPLING AND AMPULE ASSEMBLY

crystal-growing technique was used. This involved the controlled movement of an induction coil or resistance furnace in a direction so as to allow freezing to initiate at the bottom of the quartz ampule. Initial experiments utilizing viscous liquids showed that considerable cavitation was induced at the liquid-vacuum interface.

Two important points favoring the use of transparent quartz as the crucible material were:

1. The lead telluride could be sealed under vacuum, thereby allowing a simple means of protection from contamination.
2. The freezing interface could be observed during the course of an experiment.

Initial experiments demonstrated that the excessive agitation caused by the r. f. heating did not allow for a well defined rate of solidification. The vigorous stirring actually caused the molten lead telluride to be thrown up against the colder sections of the ampule wall, thereby eliminating the effects of the ultrasonic irradiation. When a moving chromel-wound resistance furnace was substituted as the heating source, the freezing procedure was much more successful.

C. EXPERIMENTAL PROCEDURE:

A two hundred (200) gram charge of equimolar quantities of lead and tellurium plus 0.03 mole % PbI_2 was initially melted in the quartz ampule container described above. After the charge was completely molten, the resistance furnace motor drive was activated. The furnace was moved in a direction so as to initiate freezing, the ultrasonic oscillations passed through the solid before reaching the liquid-solid interface. The average temperature of the molten phase was approximately $1000^{\circ}C$, as measured by a chromel-alumel thermocouple located at the crucible wall. The ultrasonic vibration transmitter was tuned to a maximum intensity at all times.

D. EXPERIMENTAL RESULTS:

The application of ultrasonic oscillations to a melt of lead telluride during solidification significantly altered the crystallization mechanism. A significant improvement in overall ingot structure such as the elimination

of columnar grain growth and shrinkage porosity was obtained. Figure 18 is a photomicrograph (88X) of the ultrasonically irradiated ingot showing a dense fine grain structure almost completely free of inclusions and gas porosity. The structure is ostensibly free of micro-cracks, inclusions, and excessive segregation. The ultrasonic irradiation also removed the columnar structure present in normally frozen lead telluride ingots. Figure 19 is a photomicrograph of an ingot of PbTe prepared in the same manner except for the elimination of the ultrasonic irradiation. The normal columnar structure is present, along with numerous micro-cracks and large amounts of segregation in the grain boundaries. This segregated phase, along with the included particles, is more easily seen in Figure 19B. The ultrasonic irradiation process produced a product which was superior to both the extruded (Figure 20)* and the cold pressed and sintered material (Figure 21)† which contained large quantities of oxide inclusions and gas porosity, making them extremely susceptible to oxidation damage at elevated temperatures. As previously reported, one of the major limitations to the use of lead telluride for power generation is its extreme susceptibility to oxidation even at low oxygen potentials. The non-porous inclusion-free structure of the irradiated ingot makes it inherently more resistant to high temperature oxidation than PbTe fabricated by extrusion or powder metallurgical techniques. Large amounts of foreign matter, such as oxides are retained in the extruded product, whereas they are agitated up to the surface of the melt in the ultrasonic casting process. The polishing and etching technique used in this study for lead telluride is given in Appendix II.

E. THE THERMOELECTRIC PROPERTIES

The efficiency of a thermoelectric generator is related to the material's properties through the figure of Merit $Z = \frac{\alpha^2}{\rho_T K_T}$ where α = the Seebeck coefficient K_T = the thermal conductivity and ρ_T the resistivity.

To compare the thermoelectric efficiency of ultrasonically prepared lead

* Acquired from Transitron Electronics Corporation

† Acquired from Minnesota Manufacturing & Mining Corporation

A.



B.

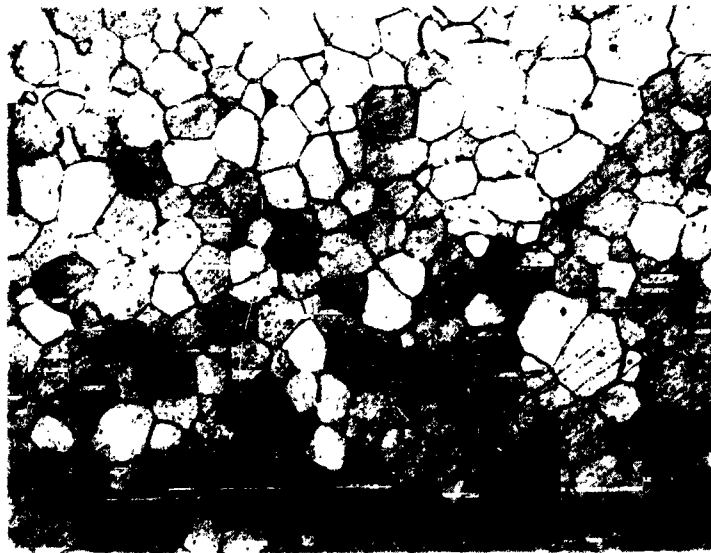
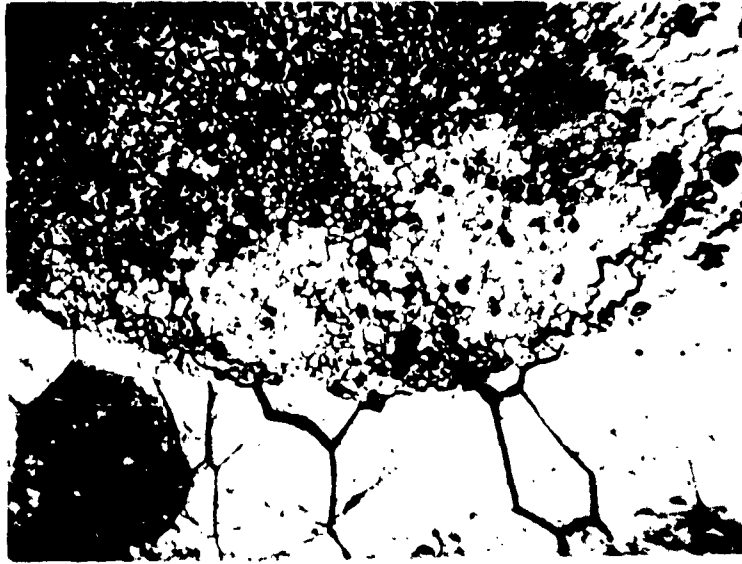


FIGURE 18 - PHOTOMICROGRAPHS OF ULTRASONICALLY IRRADIATED
INGOT
(A - 18 X; B - 88 X)

A.



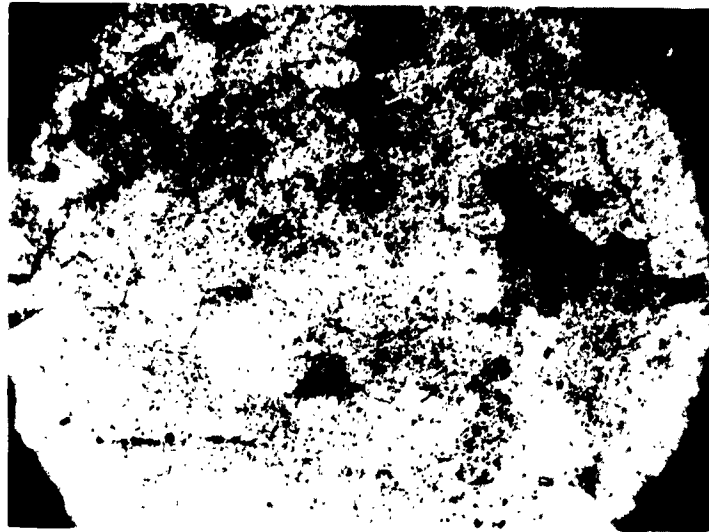
B.



FIGURE 19 - PHOTOMICROGRAPHS OF DIRECTIONALLY SOLIDIFIED
INGOT

(A - 18 X; B - 88 X)

A.

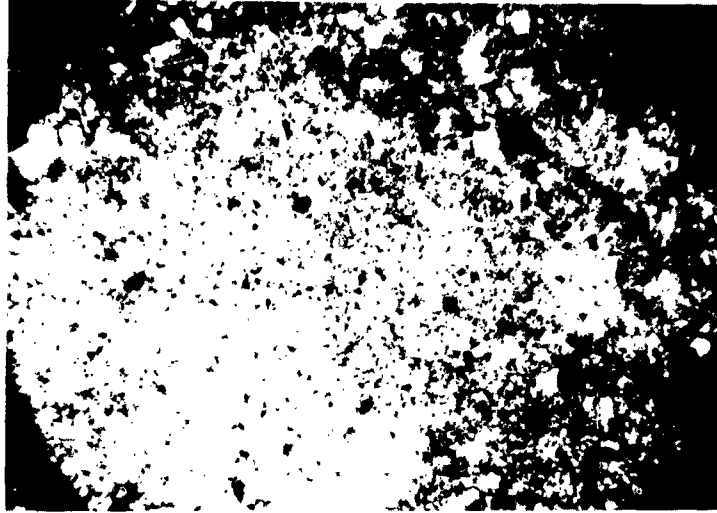


B.



FIGURE 20 - PHOTOMICROGRAPHS OF EXTRUDED PbTe (A-18X: B-88X)

A.



B.

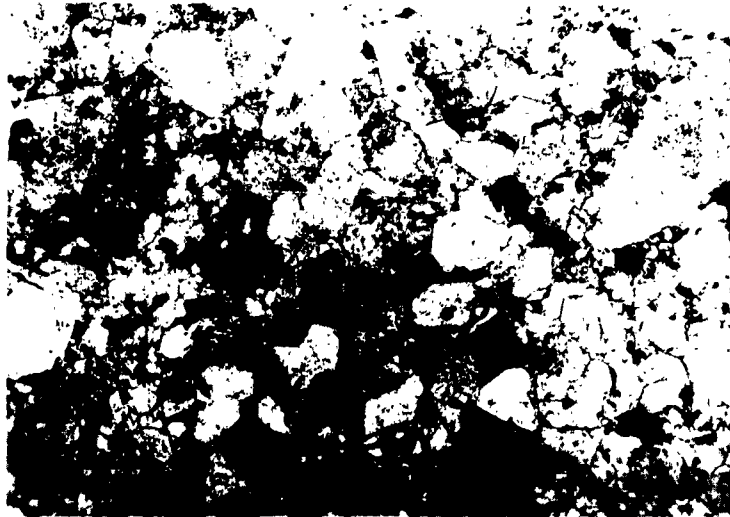


FIGURE 21 - PHOTOMICROGRAPH OF COLD PRESSED AND SINTERED
PbTe
(A - 18 X; B - 88 X)

telluride with that of extruded and cold pressed material the following properties were determined:

1. Resistivity as a function of temperature.
2. Seebeck coefficient as a function of temperature.

The relative simplicity of normal casting makes it the most attractive technique for fabricating lead telluride thermoelements. Under normal casting procedures, however, the PbTe system exhibits extreme segregation, thereby producing an inhomogeneous final product. Since the electrical properties of the thermoelement are determined mainly by the chemical composition of the element, large amounts of segregation are intolerable. In some cases long annealing treatment (10 hours at 700°C) may homogenize the structure. It is desirable, however, to eliminate this heat treatment, since extreme grain growth may accompany the process, and close control of the thermal cycle is necessary to insure the desired combination of resistivity and voltage output. We have found in as many cases as not that the segregation and columnar structure were severe enough as to render the casting unworkable. Here lies the major limitation to casting as a technique for fabricating lead telluride; that of the lack of chemical homogeneity of the final products. The experiments performed in this period have verified the hypothesis that ultrasonic agitation eliminates excessive segregation in a binary system such as PbTe. This is vividly demonstrated in Figure 22 where the room temperature resistance is plotted as a function of distance for normally directional solidified lead telluride and material solidified in the same manner under the influence of ultrasonic irradiation. It is obvious that ultrasonic agitation of the melt during solidification entirely eliminated the excessive segregation which normally manifests itself in this system. The room temperature resistivity of the ultrasonically cast PbTe (doped with 0.03 mole % PbI_2) is 0.0007 ohm-cm which corresponds favorably with the reported value 0.0005 ohm-cm for commercially available cold pressed and sintered material of the same composition. The value reported for commercially available extruded material is 0.00045 ohm-cm (doping concentration not reported). The room temperature Seebeck coefficient as measured at the top, center, and bottom of the directionally solidified

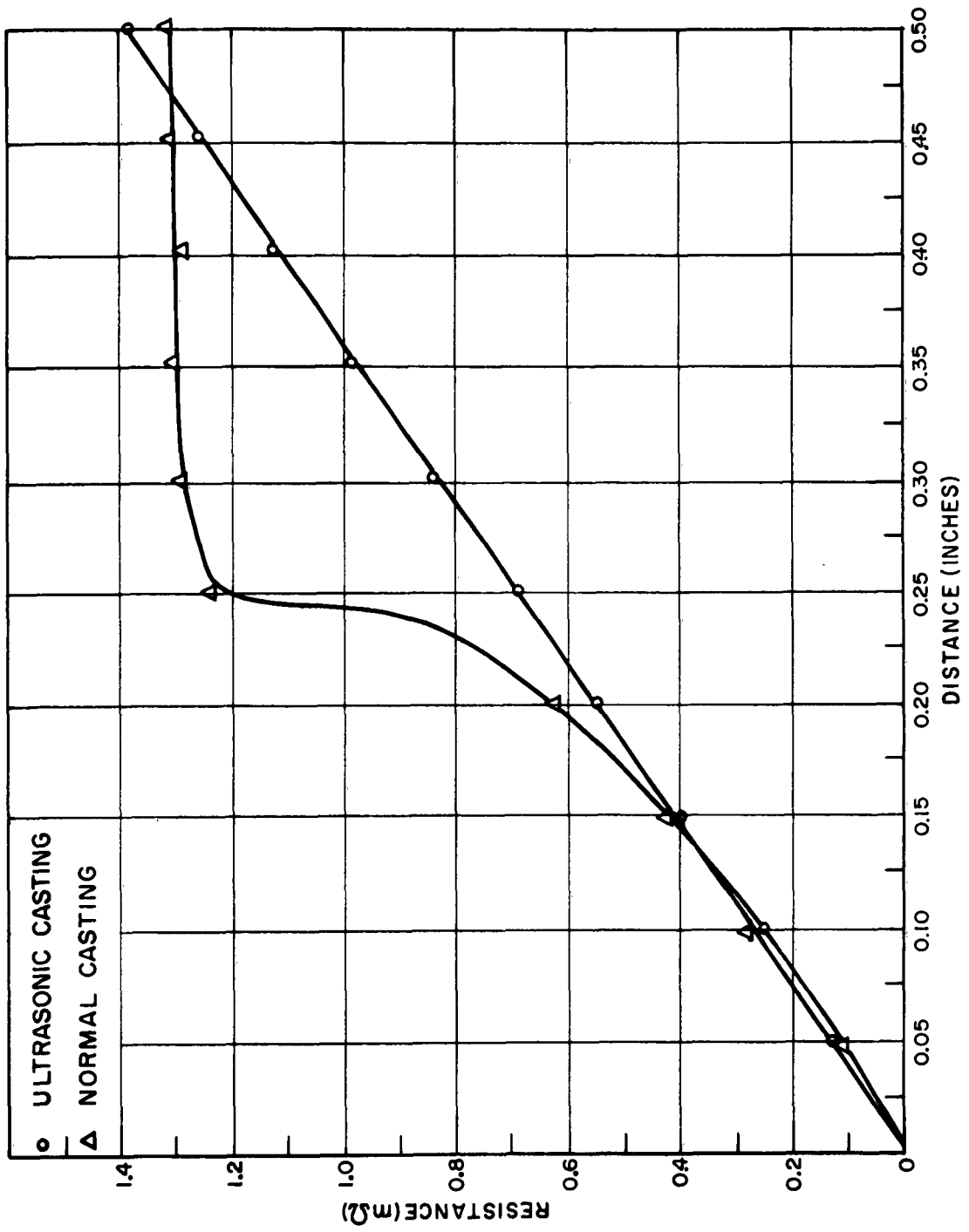


FIG. 22 RESISTANCE AS A FUNCTION OF DISTANCE

ingot and the ingot solidified under the influence of ultrasonic oscillations is given in Table 4 along with the values obtained in this laboratory for commercially available material. The absence of segregation in the ultrasonically irradiated material is again evident. The apparent change of Seebeck coefficient along the ultrasonically prepared bar is not significant when one compares it with normal limits of error of this measurement.

The effects of a high temperature anneal on the electrical characteristics of the ultrasonically prepared PbTe were investigated. After heating in an argon atmosphere for 4 hours at 700°C the room temperature resistivity and Seebeck coefficient were lowered to 0.00035 ohm-cm and 153 micro-volts per °C, respectively. Further annealing at 700°C for 10 hours produced no further change in properties. The affect of annealing was attributed to the removal of slight amounts of strain which were incorporated during the freezing process.

F. ELECTRICAL PROPERTIES AS A FUNCTION OF TEMPERATURE:

1. Resistivity:

The resistivity as a function of temperature for PbTe fabricated by extrusion, cold pressing, and sintering, and directional solidification under the influence of ultrasonic oscillations is given in Figure 23. The data shown is for N-type PbTe doped with 0.03 mole % PbI_2 . It is apparent that for a similar doping level the resistivity of the material solidified under ultrasonic agitation was considerably lower than that of PbTe processed by the other available techniques. When the solidified sample was cold worked 45% in compression the resistivity rose rapidly. The excessive increase in resistivity was due either to the formation of multiple micro-cracks, giving rise to a bulk resistivity effect, or to segregation of impurity atoms at dislocation sinks.

2. Seebeck Coefficient:

The voltage output and the corresponding Seebeck coefficients are given as a function of temperature in Figure 24 and 25, respectively. The Seebeck coefficient was obtained by measuring the slope of the voltage - output temperature curve at the temperature in question. It may be seen

TABLE 4

ROOM TEMPERATURE SEEBECK COEFFICIENTS

TYPE	*Room Temperature Seebeck Coefficient (μ V/ $^{\circ}$ C) Position		
	<u>Top</u>	<u>Center</u>	<u>Bottom</u>
Ultrasonic Casting	183	197	208
Normal Casting	38.2	67.4	89.0
Extrusion		134	
Cold Pressed and Sintered		150	

* $T_C = 4^{\circ}\text{C}$

$T_h = 17^{\circ}\text{C}$

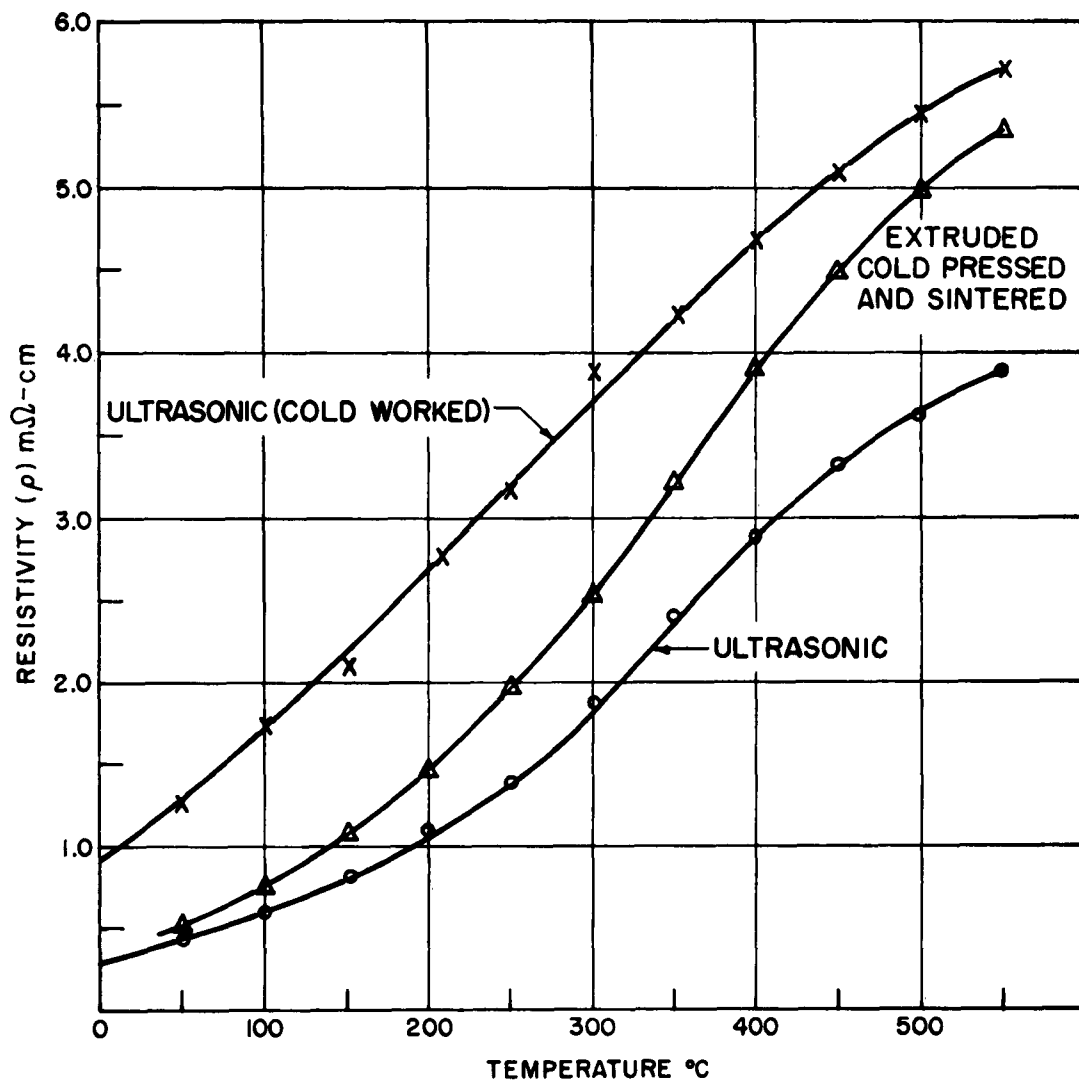


FIG. 23 RESISTIVITY OF N-TYPE PbTe AS A FUNCTION OF TEMPERATURE

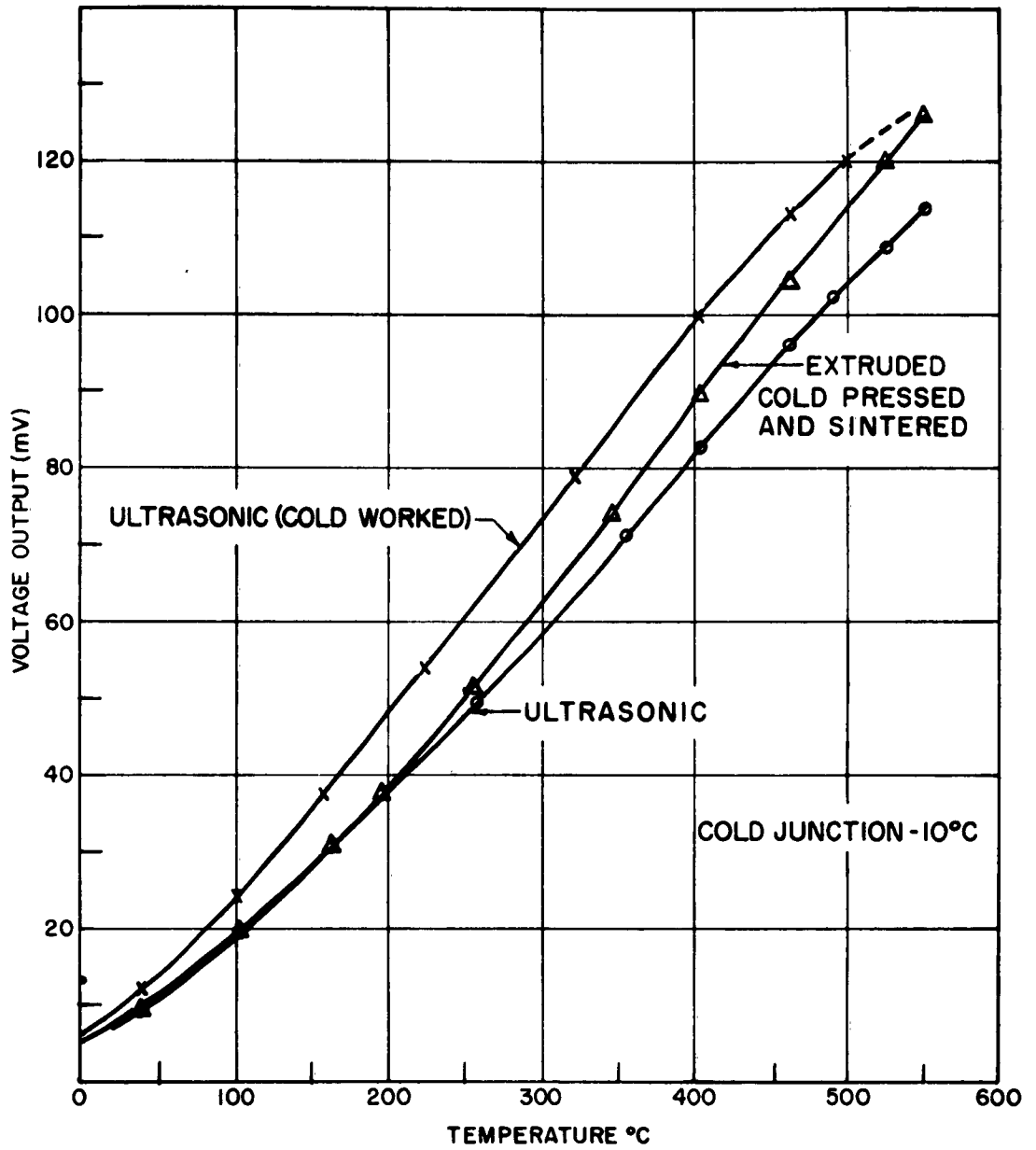


FIG. 24 VOLTAGE OUTPUT OF N-TYPE PbTe AS A FUNCTION OF HOT JUNCTION TEMPERATURE

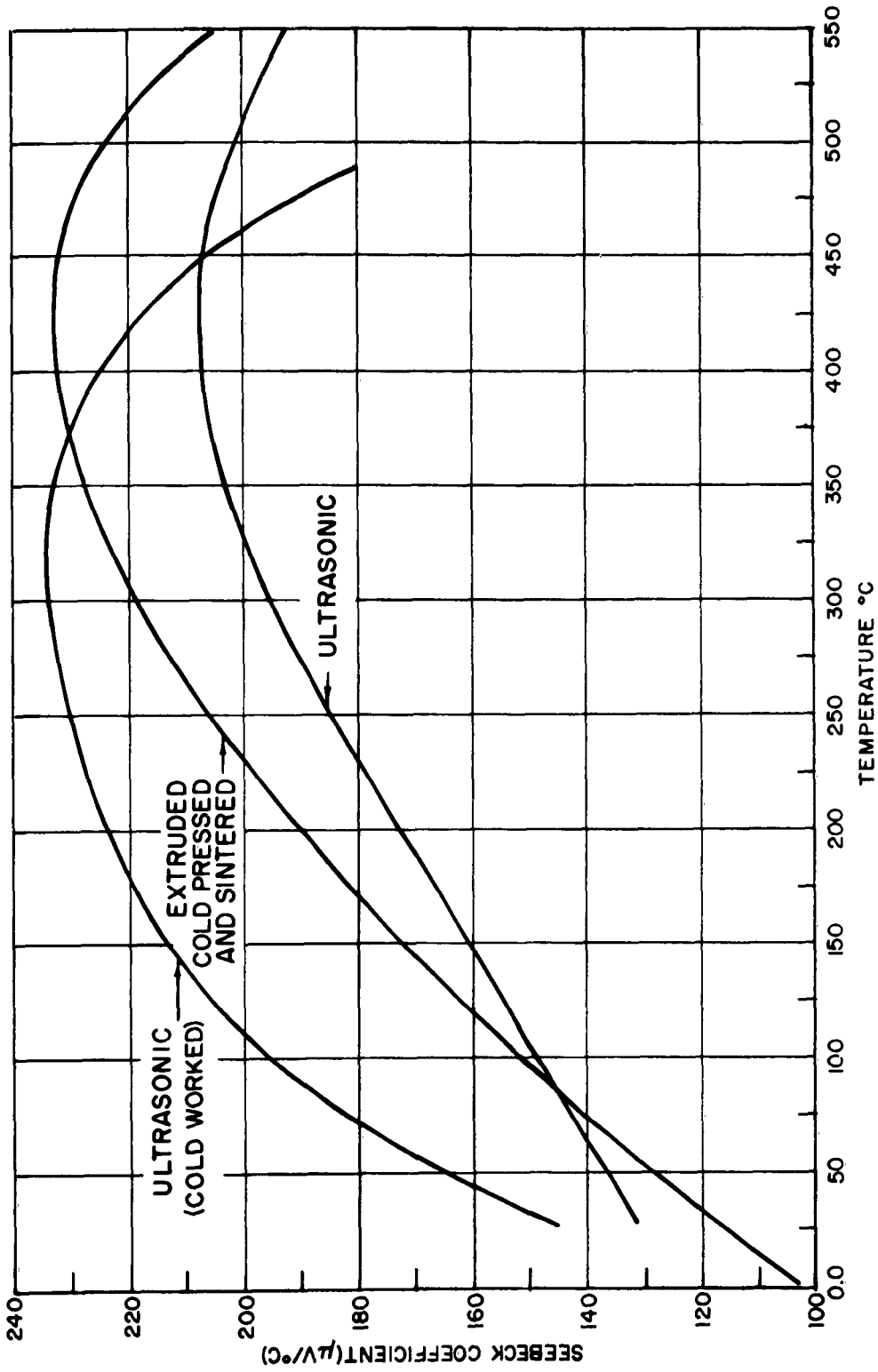


FIG. 25 SEEBECK COEFFICIENT OF N-TYPE PbTe AS A FUNCTION OF TEMPERATURE

that the maximum Seebeck coefficient of the cold worked sample falls approximately 100°C below that of the other samples tested. Since the effect of 45% cold work on the electrical properties of 0.03 mole percent PbI_2 doped PbTe is similar to that which would be obtained if the doping concentration were decreased by approximately 0.015 mole percent PbI_2 , it appears as if impurity segregation is the mechanism by which the electrical properties are altered. The character of the Seebeck coefficient-temperature relationship is similar for the extruded, cold pressed and sintered and the directionally solidified ultrasonically irradiated PbTe, the latter material exhibiting a slightly lower coefficient.

3. Electrical Efficiency

The factors α^2/ρ for the various materials studied are given in Figure 26. The electrical efficiency of materials solidified under the influence of ultrasonic oscillations is slightly higher than that of the others. It should be kept in mind, however, that the electrical properties of PbTe produced by each technique may be altered considerably by slight changes in the initial PbI_2 concentration. A study of the concentration variable would be necessary before any definite statement could be made as to the advantages or disadvantages, on an electrical basis, of material prepared under the influence of ultrasonic oscillations. The main point to be made, however, is that the electrical properties of PbTe fabricated by the before-mentioned technique are at least equivalent to those of cold pressed and sintered and extruded material.

G. MECHANICAL PROPERTIES OF N-TYPE PbTe:

The mechanical properties of N-type PbTe have been investigated. The experimental results consist mainly of room temperature compressive flow curves for polycrystalline cylinders of various grain sizes and structural perfection. The data will be analyzed in terms of their effect upon the ductility and ultimate compressive strength of lead telluride thermoelements. The compression tests were performed on a Hounsfield Tensometer.

1. Ductility

The stress-strain relationships for extruded, cold pressed and sintered, directionally solidified, and ultrasonically irradiated PbTe are

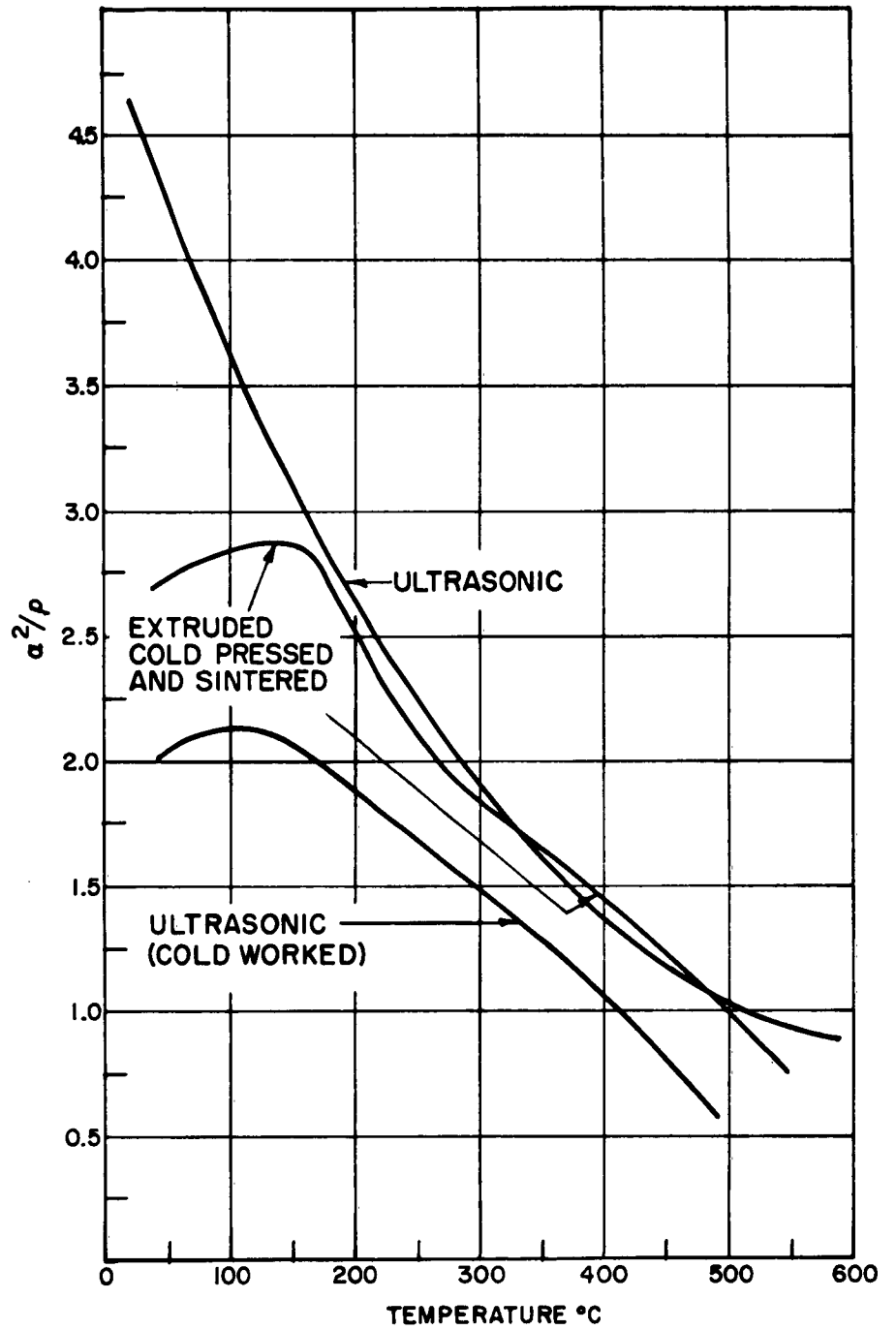


FIG.26 ELECTRICAL EFFICIENCY FACTOR (α^2/ρ) FOR N-TYPE $PbTe$ AS A FUNCTION OF TEMPERATURE

given in Figure 27. It may be seen that the cylinders solidified under the influence of ultrasonic oscillations possess much greater ductility than the material processed by the other techniques. (The stress-strain relationships for ingots, 4, 5, and 7 were eliminated from the curve since they all coincide with the reported curve; the ultimate stress and strain for these ingots are denoted on Figure 27 by triangles.)

The extremely fine-grained cylinder solidified under the influence of ultrasonic oscillations gave a reduction in length of nearly 50% before fracture occurred at a stress of 24,450 psi (in compression). This improved room temperature ductility can be attributed to the removal of microscopic and macroscopic impurities from the structure. The removal of impurities is accomplished by the ultrasonic agitation which causes inclusions which are normally entrapped in the freezing ingot to be levitated at the surface of the melt. The main effect of the impurities (oxide gases, etc.) is to act as barriers to slip, thereby limiting the amount of elongation possible for a specific stress. A careful metallographic examination of the resultant structures verified the relative absence of impurities and inclusions in the ingots prepared by the ultrasonic technique.

The extremely limited room temperature ductility of extruded PbTe is a result of the large amount of previous strain hardening imparted to the material by this procedure. In this case, the majority of dislocations are tied up, thereby allowing only a minimum amount of further deformation. The observable decrease in length of the cold pressed and sintered material appeared to be largely a compaction effect; the material being initially only 95% of theoretical density.

2. Ultimate Compressive Strength:

Table 5 contains the ultimate compressive strength and grain size for the lead telluride cylinders tested. The data in all cases (except for the cold pressed and sintered material) indicates an inverse relationship between grain size and ultimate compressive strength. The inconsistent behavior of the cold pressed and sintered material was a consequence of its mechanism of failure. Fracture took place in this case by what appeared to be a complete collapse of particle cohesion, whereas all other samples failed in a brittle manner by a mechanism which involved intergranular fracture.

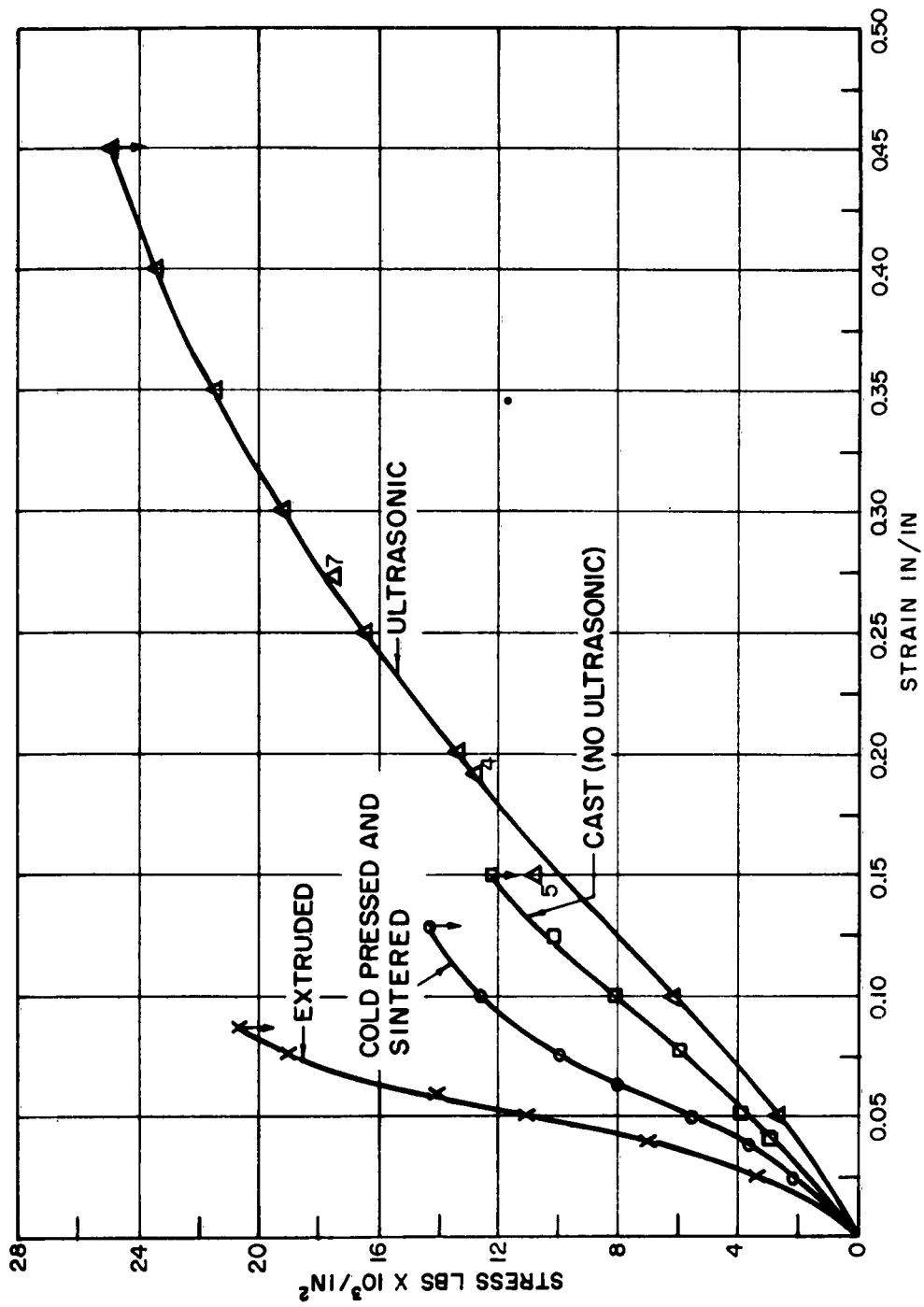


FIG. 27 STRESS-STRAIN RELATIONSHIP (COMPRESSION) FOR N-TYPE PbTe

TABLE 5

Ultimate Compressive Strength (to Fracture) and Grain
Size of N-type PbTe (Room Temperature Test)

<u>Sample</u>	<u>Compressive Strength PSI x 10⁻³</u>	<u>Average Grain Diameter inch x 10⁻³</u>
1. Cast (ultrasonic agitation)	24. 41	3
2. Extruded	20. 75	21
3. Cold pressed and sintered	12. 9	5
4. Cast (ultrasonic agitation)	10. 8	144
6. Cast (ultrasonic agitation)	17. 4	45
7. Cast (no ultrasonic agitation)	12. 2	60*

* Grain size variable. Columnar structure present.

The increase in ultimate strength with a decrease in grain size may be discussed simply in terms of a mechanism which involves the propagation of intercrystalline micro-cracks through the polycrystalline aggregate. The higher ultimate stress observed for the fine-grained material may be attributed to its increased resistance to intergranular micro-crack propagation.

H. HOT PRESSING OF LEAD TELLURIDE

Some experiments were performed on the hot pressing of 0.03 mole percent PbI_2 doped PbTe . The components were initially fused together in a sealed quartz capsule. They were then heat treated just below the liquidus for two hours before air quenching. The room temperature thermoelectric properties were then measured mostly as a check on homogeneity. The alloy was then crushed so that 70% was at 325 mesh, 20% at 200 mesh, and 10% at at 120 mesh. The three fractions were then blended and hot pressed in a graphite dye at 600°C at a pressure 1000 psi. The resulting specimens were 100% dense with very fine equiaxial grain structure, as shown in Figure 28. It is interesting to note that the grain size appears to be uniform throughout the sample and bears no resemblance to the original particles used. Complete interdiffusion between particles has taken place with subsequent recrystallization. The room temperature properties of the hot pressed material were as follows:

$$\begin{aligned}\alpha &= 111 \text{ micro-volts } / ^\circ\text{C} \\ \rho &= 0.0002 \text{ ohm-cm}\end{aligned}$$

Since the ultrasonic technique appeared inherently more interesting, the hot pressing study was discontinued in favor of the former.

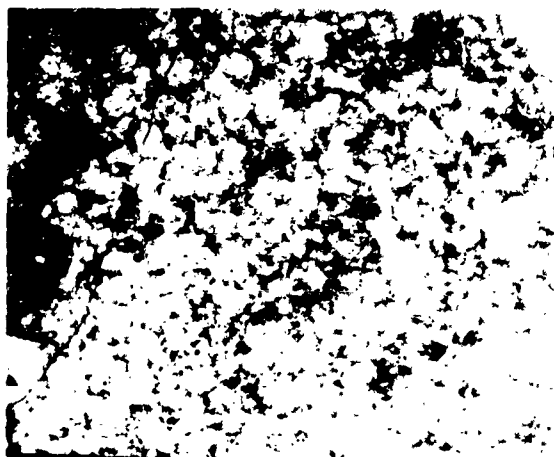


FIGURE 28 - PHOTOMICROGRAPH OF HOT PRESSED PbTe (75 X)

IV. EFFECTS OF THERMAL GRADIENTS

This study was undertaken in order to determine the limits of acceptable temperature gradients for P and N-type lead telluride, bonded to conductive electrodes. Since no previous data were available, an initial study was also made in order to determine acceptable temperature gradients for unbonded lead telluride.

A. EXPERIMENTAL EQUIPMENT

Figure 29 shows an apparatus which was constructed for the thermal testing of thermoelectric elements. A radiant source was used to heat one face of the sample, while the other was mounted on a water-cooled pedestal by means of silver paste. The pedestal was hermetically enclosed in a pyrex vessel which was provided with a plain window and with means for evacuating and back-filling with inert gas. The cold junction temperature of the sample was measured by means of a copper-constantan thermocouple. A pointed tungsten wire which was lightly pressed against the hot face of the sample was used to measure the hot junction temperature by means of the generated voltage output. A check on the uniformity of the temperature of the hot face was made by scanning it with a focused beam and recording the voltage output. It was found that the temperature was uniform to within the experimental error of a few degrees Centigrade over about one (1) cm².

B. EXPERIMENTAL RESULTS

Several samples of cold pressed and sintered PbTe both N and P-type, and TLI sample #712 N-type hot pressed have been tested. These tests consisted of heating the end face of the sample to a high temperature for an arbitrary length of time, while keeping the other face of the sample at a low temperature by cooling the pedestal. All the samples tested were subjected to a temperature gradient in excess of 1000°C per cm. No cracking of the samples was observed and no increase in resistivity (measured at room temperature), or decrease of the average Seebeck coefficient was observed. Table 6 summarizes some of the test results.

Since the unconstrained lead telluride was found to withstand extremely high temperature gradients, work was initiated to determine the behavior of bonded thermoelements. Figure 30 and 31 show that the results of several

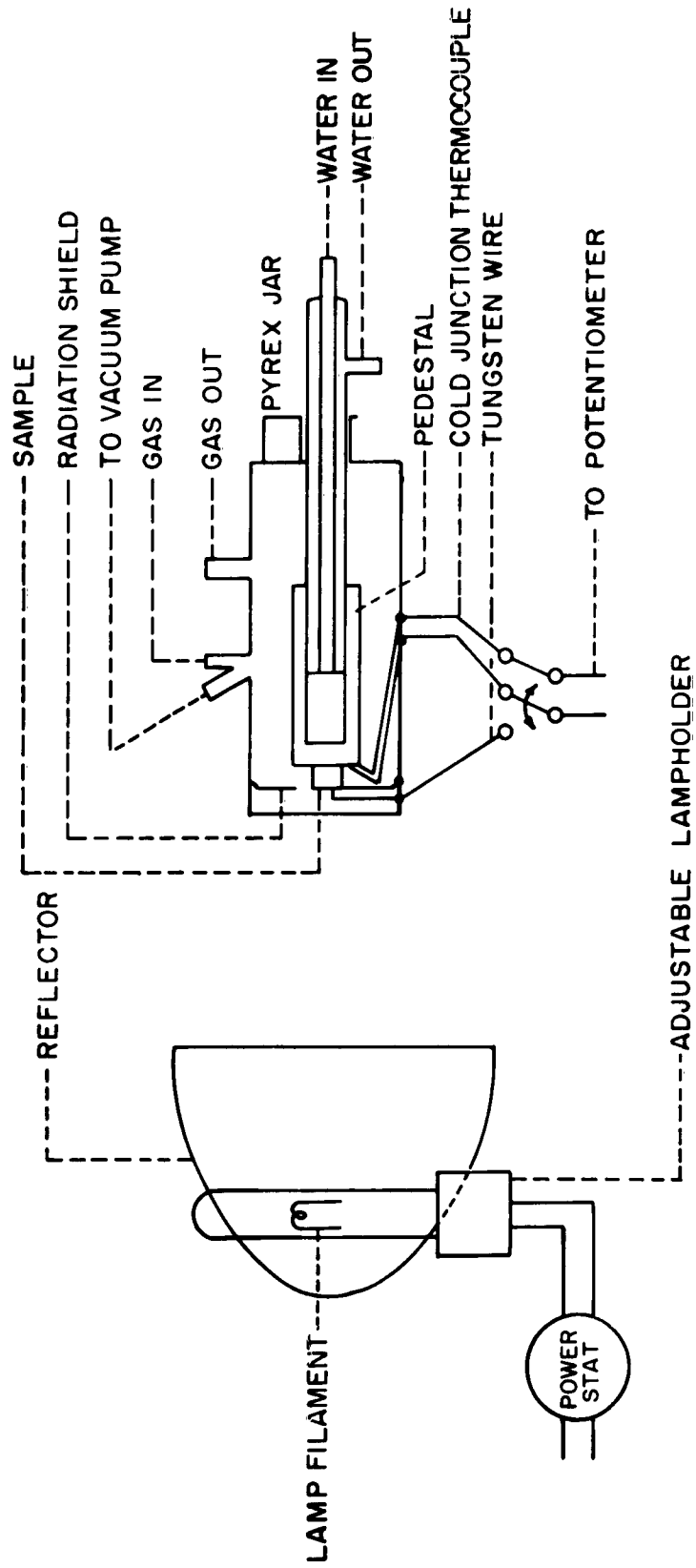


FIG. 29 SCHEMATIC OF THERMAL TESTING APPARATUS

TABLE 6 - Thermal Gradient Test Results:

Material	Thermal Gradient °C	Time	Average Seebeck Coefficient $\mu V/^\circ C$ Before Test	Average Seebeck Coefficient $\mu V/^\circ C$ After Test	Resistivity at Room Temp. milliohm-cm Before Test	Resistivity at Room Temp. milliohm-cm After Test	Remarks
Pressed and Sintered P-type 1/4" dia. x 1/4" thick	380°	20 min.	231.6	235.2	0.22	0.22	No physical change.
	605°	20 min.					
	700°	20 min.					
Pressed and Sintered N-type Dimensions 1/4" dia. x 1/4" thick	275°	20 min.	215.	218.7	0.23	0.24	No physical change.
	480°	20 min.					
	600°	3 hrs.					
M. R. L. #71-2 1/4" square x 1/8" thick	550°	1 hr.	192.3	190.2	0.26	0.26	No physical change.
	600°	2 hrs.					

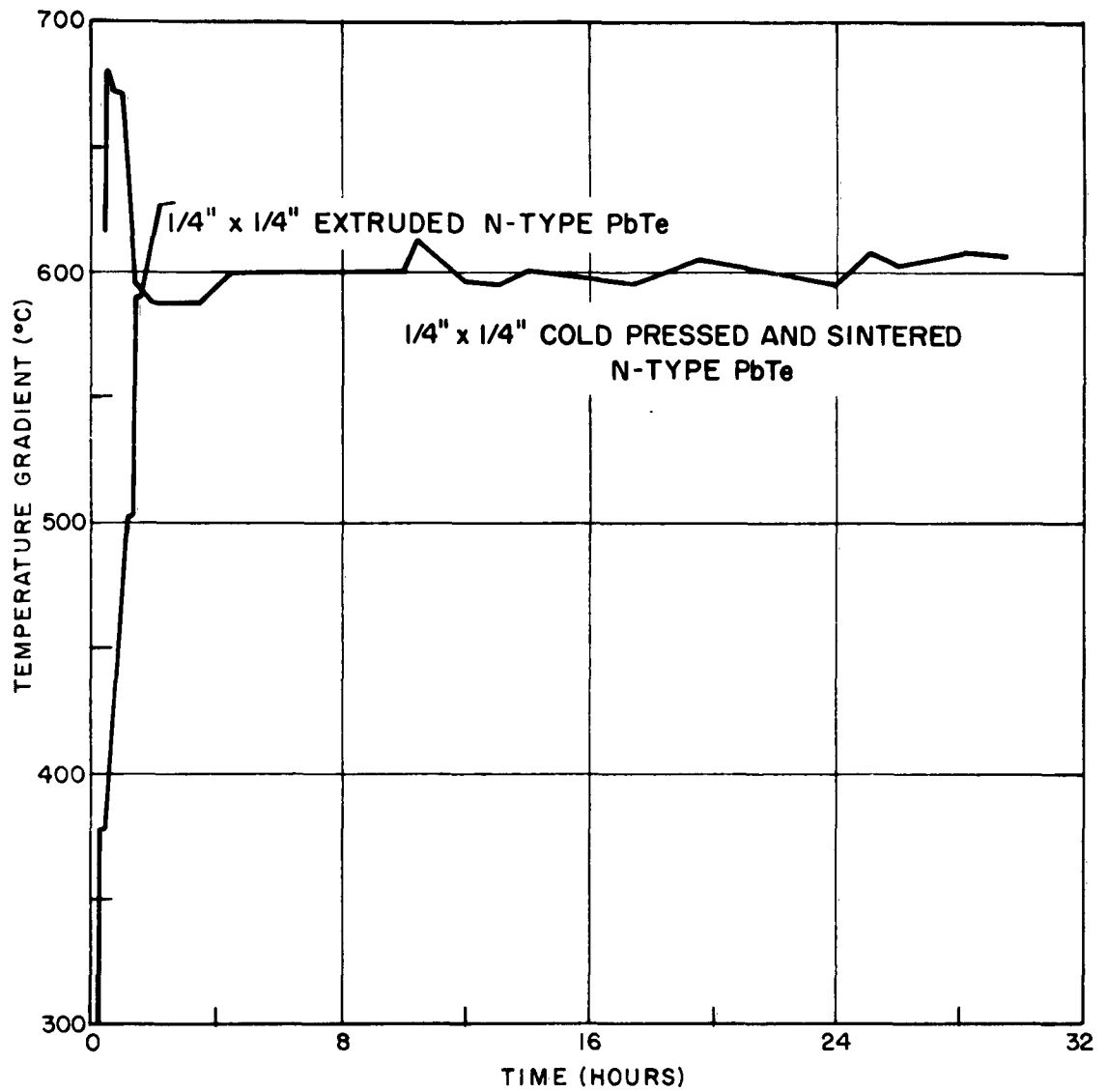


FIG. 30 LIFE TEST OF N-TYPE LEAD TELLURIDE
-55-

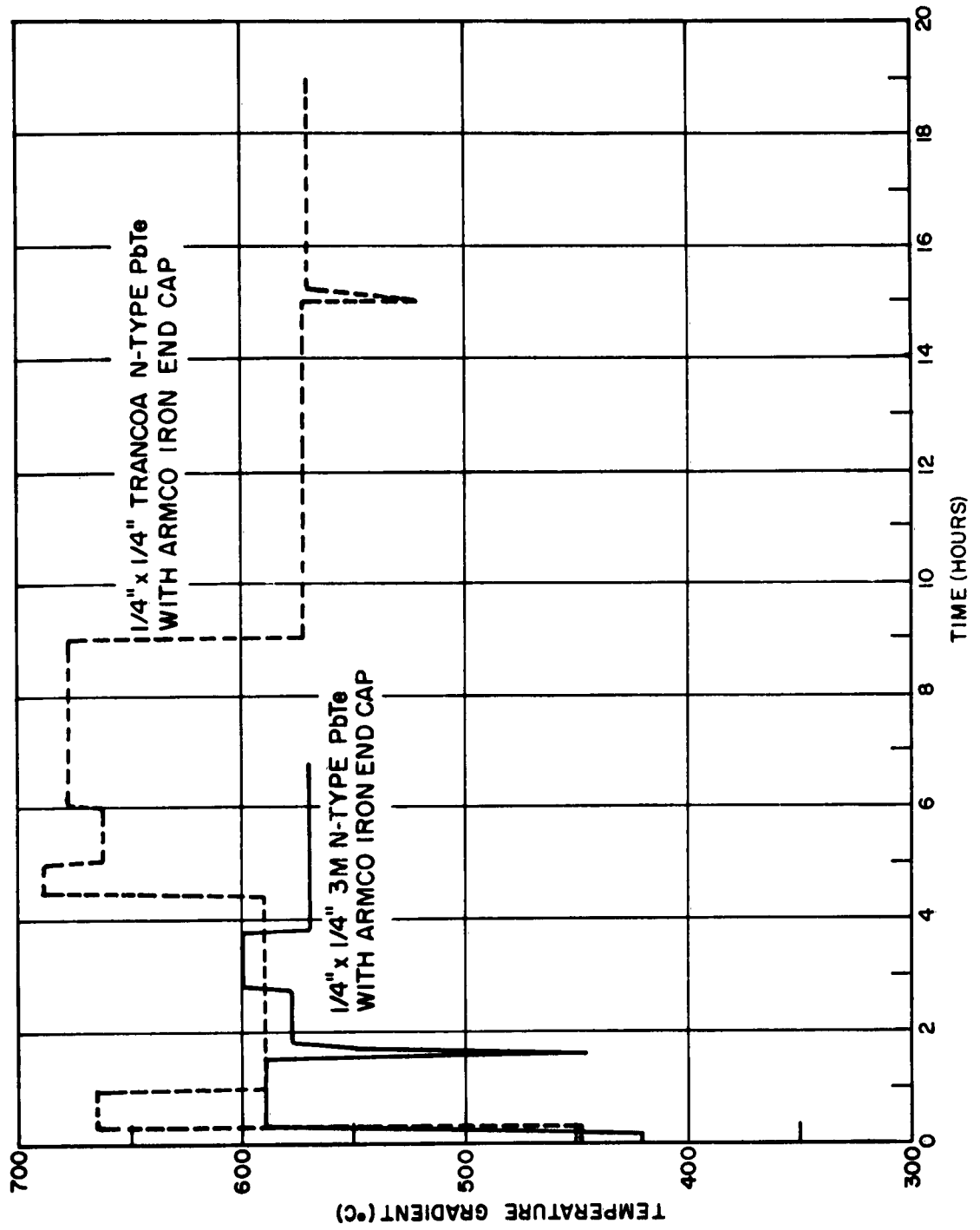


FIG. 31 LIFE TEST OF BONDED N-TYPE PbTe

hours of thermal gradient testing of both bonded and unbonded samples of N-type PbTe. Careful metallographic examinations of the specimens after thirty hours of testing showed no crack development or grain growth. A bonded sample of N-type lead telluride was tested for over 250 hours. During the first 15 hours the thermal gradient in the sample was 580°C . During this period the average Seebeck coefficient dropped approximately 3%. However, when the thermal gradient was reduced to a more realistic value of approximately 510°C no further deterioration of the sample was observed.

As far as could be ascertained from the limited number of tests completed, the bonded lead telluride thermoelements appeared to be able to support a temperature gradient of approximately 510°C , (1/4 inch x 1/4 inch thermoelement). The major problem, as far as long time service is concerned, appears to be the extreme susceptibility of the bond to oxidation damage. It is evident, therefore, that in order to utilize a bonded thermoelement of the previously mentioned type a suitable encapsulation process for the bond region is necessary. Further investigations should be directed toward this end.

V. SUMMARY

1. A technique which utilizes a SnTe braze, has been developed for bonding P and N-type PbTe to pure Fe electrodes. Contact resistances fall in the range of 5 - 15 micro-ohm-cm².

2. A bonding technique involving the interdiffusion of Fe and N-type PbTe at 850°C has been developed. Contact resistances fall in the range of 10 - 20 micro ohm-cm².

3. N-type PbTe directionally solidified under the influence of ultrasonic oscillations has been found to possess superior mechanical properties to presently available material.

4. Bonded and unbonded PbTe (1/4" x 1/4" D) were found to be capable of sustaining, without any visible damage, a temperature gradient of 510°C for over 250 hours.

5. The major problems, as far as long-time service is concerned, appear to be:

- (1) The instability of Na-doped P-type PbTe.
- (2) Extreme susceptibility of the bond region to oxidation.

VI REFERENCES

1. E. W. Bollmeier, Direct Conversion of Heat to Electricity, edited by Joseph Kaye and John A. Welch (John Wiley and Sons, Inc., New York, 1960, p 46-1.
2. M. Weinstein and A. I. Mlavsky, Review of Sci. Inst. Vol. 33, No. 10, 1119 - 1120, October 1962.
3. M. Hansen and K. Anderko, Constitution of Binary Alloys, (McGraw-Hill Book Company, Inc., New York, 1958), p 1209.
4. P. H. Schmidt, J. Elect. Soc., 109, 879 (1962)
5. M. K. Norr, J. Elect. Soc., 109, 433 (1962)

VII. APPENDIX I - DETAILED DESCRIPTION OF BONDING PROCESS

A. DIFFUSION BONDING OF N-TYPE LEAD TELLURIDE:

This process comprises the interdiffusion of PbTe and Fe (Armco) into each other at a temperature below the Fe-PbTe eutectic of 874°C

1. Preparation of Parts to be Bonded:

Both the PbTe thermoelement and the iron electrodes were lapped on their contact surfaces with fine emery paper (1-O Carborundum) and then ultrasonically washed in successive batches of trichlorethelene until clouding of the solvent was no longer visible. Absolute cleanliness was essential for suitable bonding.

2. Bonding:

The parts were loaded in a simple carbon jig made from semiconductor grade high purity carbon with a dead weight axial loading of 200 grams for a 1/4 inch diameter thermoelement. The jig was placed in a tube furnace under an argon atmosphere, which was very pure with respect to oxygen. It was necessary to evacuate the furnace tube three to four times along with intermediate argon flushing. The argon used contained no more than 1 part per million of oxygen. (The atmosphere was considered suitable for bonding if the iron electrodes did not oxidize at temperature.) The furnace temperature was run up at the rate of about 2°C per minute to a temperature at the jig of $858 \pm 2^\circ\text{C}$, it was held at this temperature 30 minutes and then allowed to furnace cool. Cool-down time was approximately 1 to 1.5 hours.

3. Results:

The bonded pieces showed no signs of oxidation. The bond region comprised both diffusion of iron into lead telluride and of some species, probably lead, into the iron. The contact resistance was less than 10 micro-ohm-cm² in general. If the junctions showed higher resistances, this was normally due to poor sample preparation, inadequate jiggling, or an improper atmosphere. The bond obtained was mechanically stronger than the lead telluride itself.

B. BRAZE BONDING OF P-TYPE LEAD TELLURIDE:

1. Preparation of Parts to be Bonded

The lead telluride bond and the iron (Armco) electrodes were prepared as described above by lapping and ultrasonic washing.

2. Preparation of SnTe

Stoichiometric amounts of ultra-pure Sn and Te were sealed in an evacuated quartz capsule. The capsule was heated above 808°C and after the whole mass was molten and the elements had reacted completely, the melt was allowed to solidify. It was then zone leveled at least ten times to insure homogeneity. It was found necessary to prepare the tin telluride with great care. A determination of the melting point of SnTe was made and revealed a value of $805 \pm 3^{\circ}\text{C}$. This value was higher than reported in the literature. Failure to zone level adequately resulted in an inhomogeneous mass, the melting point of any part of which was less than 805°C .

3. Alloying SnTe To Electrodes:

The cleaned electrodes were placed in depressions in a carbon jig, and chunks of the SnTe were placed on each. A sufficient excess of the alloy was used so as to insure complete coverage to a depth of 10 mils or more. The jig was then heated in a tube furnace in a pure argon atmosphere to 850°C , and left at this temperature for about two hours. The jig was then cooled to room temperature in argon by sliding the tube out of the furnace. Cool down time was approximately 20 minutes.

4. Preparation of Electrodes:

The iron disks were waxed onto a steel plate as preparation for surface grinding of the excess SnTe. The disks were ground so as to leave two to four mils of SnTe on the iron substrate. The electrodes were then removed from the plate and carefully cleaned using ultrasonic agitation of the solvents.

5. Bonding:

The parts to be bonded, i. e., two electrodes plus one PbTe thermoelement were placed in a carbon jig using a dead weight axial loading of about 25 grams (for 1/4 inch diameter pieces.). A carbon disk spacer was

used between the upper electrodes and the stainless steel weight. The jig was then heated for 2 to 5 minutes in a tube furnace to 808°C using all the precautions described above to insure an oxygen-free atmosphere. The jig was then cooled to 700°C, held there for one hour and then cooled rapidly to room temperature (cool-down time about 20 minutes.)

6. Results:

Microscopic examination of the bond region showed the following:

1. Intergranular penetration of SnTe alloys into the bulk iron.
2. A solid solution region of SnTe-PbTe approximately 3 to 5 mils.

No second phase was observed in this region.

When great care was not taken in preparing the bond and the bond materials, the SnTe rich region was found to be porous and to contain what appeared to be oxide inclusions. This resulted in high contact resistances compared with the attainable values of less than 10 micro-ohm-cm². As would be expected, the susceptibility of the bond region to oxidation was greatly enhanced by porosity. SnTe again is an excellent brazing material. The bond region is mechanically stronger than the lead PbTe itself.

VIII. APPENDIX 2 - CHEMICAL POLISH AND ELECTROLYTIC ETCH FOR PbTe

There have been many polishing and etching techniques reported for PbTe. Most of these have been developed for optical measurements or microstructural observations. We have found that for macrostructural observation a combination of a chemical polish described by Schmidt (4) and a modification of an electrolytic etch described by Norr (5) gives satisfactory results. The electrolytic technique has also been used for polishing purposes. We have found, however, that scratch removal and subsequent etching performance are improved by use of the chemical polish.

A short description of the process used in this study follows:

A. CHEMICAL POLISH:

1. First prepare sample by abrading the surfaces with water lubricated 2/0 emery paper.
2. Abrade on 4/0 emery paper.
3. Polish on cotton cloth impregnated with a solution of 50% H_2O_2 (H_2O_2 30%), 50% glacial acetic acid and Linede A abrasive (hand operation on stationary cloth).
4. Polish in similar manner without abrasive.

B. ELECTROLYTIC ETCH:

1. Place in electrolytic etch kit containing electrolyte solution prepared by mixing
 - (a) 20 g KOH pellets in 45 ml distilled H_2O ;
 - (b) Stir in 35 ml of glycerol and 20 ml of ethanol.
2. Use platinum foil as one electrode.
3. PbTe with surface in horizontal plane as other electrode.
4. Electrolyte was stirred at 100 r. p. m.
5. Make PbTe cathode and Pt anode - polish for 15 seconds at 4 volts to remove remaining scratches.
6. Rinse in H_2O to remove purple-black film.
7. Reverse polarity and etch by using a cell voltage of 1 volt for 1 minute.
8. Rinse in H_2O .

Grain structure and various inclusions should be clearly visible if care is taken to remove any foreign material from electrolyte. The electrolyte must be changed frequently since a blackened solution always produces poor surfaces.

IX. TECHNICAL CONTRIBUTORS

A. I. MLAVSKY

H. STROP

M. WEINSTEIN

J. AIREY

T. LEWIS

E. TOCMAN

B. SHAW

R. MC NEILL